research report

Distortional Buckling of Cold-Formed Steel Columns

RESEARCH REPORT RP00-1

AUGUST 2000
REVISION 2006

Committee on Specifications
for the Design of Cold-Formed
Steel Structural Members

American Iron and Steel Institute

The material contained herein has been developed by researchers based on their research findings. The material has also been reviewed by the American Iron and Steel Institute Committee on Specifications for the Design of Cold-Formed Steel Structural Members. The Committee acknowledges and is grateful for the contributions of such researchers.

The material herein is for general information only. The information in it should not be used without first securing competent advice with respect to its suitability for any given application. The publication of the information is not intended as a representation or warranty on the part of the American Iron and Steel Institute, or of any other person named herein, that the information is suitable for any general or particular use or of freedom from infringement of any patent or patents. Anyone making use of the information assumes all liability arising from such use.

DISTORTIONAL BUCKLING OF COLD-FORMED STEEL COLUMNS

FINAL REPORT

August, 2000

a project sponsored by:
The American Iron and Steel Institute

research completed by:
B.W. Schafer

Distortional Buckling of Cold-Formed Steel Columns

(FINAL REPORT)

August 2000

APPENDICES

LIST OF TABLES

LIST OF FIGURES

1 Executive Summary

Research on the distortional buckling of cold-formed steel columns, primarily C and Z shapes is summarized below.

Defining distortional buckling:
- involves rotation at the web/flange juncture in typical members,
- exists at half-wavelengths intermediate between local and flexural or flexural-torsional buckling.

Existing research
- shows that post-buckling capacity exists in the distortional mode,
- has opened many questions about how distortional buckling interacts with other buckling modes,
- includes examples of how other specifications have incorporated distortional buckling.

Prediction by hand methods:
- local buckling of the member may be predicted using semi-empirical interaction models (see Appendix B),
- distortional buckling may be predicted using Schafer's approach or Hancock's approach (see Appendix B).

Prevalence of the distortional mode:
- narrow flanges (compared to the web depth) and wide flanges both lead to low distortional buckling stresses,
- short lips and very long lips (lip lengths as wide as the flange width) lead to low distortional buckling stresses,
- the majority of typical C and Z members suffer more from local buckling than distortional buckling,
- in members in which additional folds are added to break up the local buckling mode, distortional buckling is much more important and prevalent.

Ultimate strength in the distortional mode
- has lower post-buckling capacity than local buckling,
- has higher imperfection sensitivity than local buckling; but
- may be predicted by simple formulas when the distortional buckling stress is accurately known.

Comparison of the AISI (1996) Specification with existing data shows
- overall performance is on average 6% unconservative, but
- the error is not specifically due to distortional buckling, rather
- systematic error exists for high web slenderness (h/t) and/or high web height to flange width (h/b) ratios,
- the error is primarily due to the element approach which ignores all local buckling interaction.

Alternative design methods using an effective width approach:
- can lead to simpler design for local buckling,
- require the addition of a distortional buckling calculation,
- provide a means for effectively designing members prone to distortional failures,
- compared to the AISI (1996) method longer lips are encouraged and short lips discouraged.

Alternative design methods using a Direct Strength approach:
- remove systematic unconservative prediction in current methods,
- agree better with available experimental data,
- avoid the use of lengthy element by element calculations,
- provide a means for rationally incorporating numerical methods and optimizing member design,
- provide an explicit design check on both local and distortional buckling limit states,
- compared to the AISI (1996) method, encourages the use of longer lips and discourages the use of narrow members (high h/b) with slender webs (high h/t) and short lips (low d/b).

Recommendations for design and the AISI Specification:
- for immediate adoption, add new commentary language for B4.2 providing limits of the current method (see Appendix F.1 for proposed wording),
- for interim adoption, remove section B4.2, replace with k = 4 solution and add a distortional buckling check (see method C1 in Appendix B and proposed specification language in Appendix F.2),
- for interim adoption as an alternative design method, and for long-term adoption, adopt the Direct Strength design method and allow rational analysis (see methods C3 and C2 in Appendix B and proposed specification language in Appendix F.3).

2 Introduction

What is distortional buckling?

Distortional buckling, also known as "stiffener buckling" or "local-torsional buckling", is a mode characterized by rotation of the flange at the flange/web junction in members with edge stiffened elements. In members with intermediately stiffened elements distortional buckling is characterized by displacement of the intermediate stiffener normal to the plane of the element. This study focuses on distortional buckling of members with edge stiffened elements. Distortional buckling may be directly studied by finite strip analysis.

Consider the finite strip analysis of a lipped C in pure compression, Figure 1. The analysis proceeds by finding the lowest buckling mode at a variety of different longitudinal half sine waves (half-wavelengths). The minima of the curve reveal different buckling modes that exist for the member. In this case, distortional buckling exists at an intermediate half-wavelength, between local buckling and long half-wavelength flexural or flexural-torsional buckling. This intermediate length is a defining characteristic of distortional buckling.

As Figure 1 shows, for a typical lipped C member in pure compression local buckling often occurs at a lower buckling stress than distortional buckling. If the local buckling stress is significantly lower than the distortional buckling stress then it is possible that distortional buckling may be safely ignored. However, many situations exist in which distortional buckling must still be considered, even in routine design.

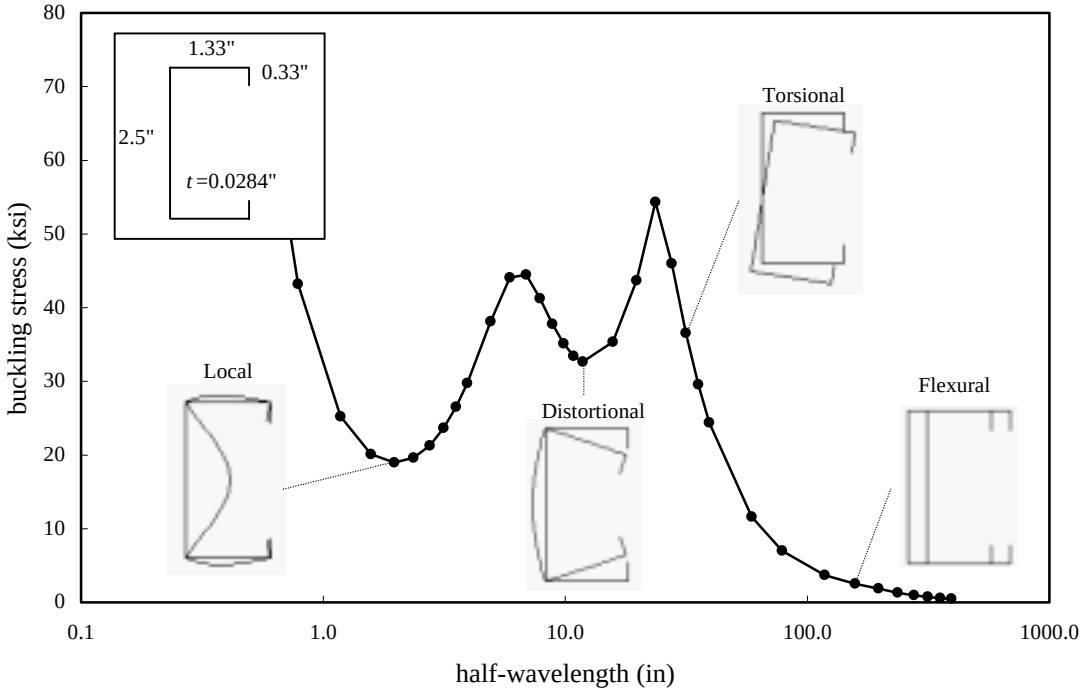

Figure 1 Finite Strip Analysis of a Drywall Stud

How does distortional buckling behave?

Intuition for local buckling behavior is a relatively straightforward – as width-to-thickness (*w/t*) ratios increase local buckling stress declines. This fact serves the engineer well in designing for local buckling. Similar intuition for distortional buckling is difficult to arrive at. A series of examples examining the distortional buckling stress of lipped C columns are summarized in Figure 2. (The distortional buckling stress was calculated using closed-form expressions derived in Schafer (1997), examples of this method are given in Appendix B). Figure 2 provides a means to develop a modest amount of intuition with respect to distortional buckling.

For distortional buckling:

Too little or too much flange is not good: Figure 2 (a) and (b) show results as the flange width is varied. In the examples, the highest distortional buckling stresses are achieved around a *b/h* ratio of 1/3; this conclusion is not general though, as different stiffener lengths yield a different optimum *b/h* (where *b* = flange width, *h* = web height and *d* = lip length). If the flange is too narrow local buckling of the web is at wavelengths near distortional buckling of the flange and the distortional mode easily forms at low stresses. If the flange is excessively wide local buckling is not the concern, but rather the size of the stiffener required to keep the flange in place is the concern. For practical stiffener lengths, wide flanges also lead to low distortional stresses.

Longer lips are usually better: Figure 2 (c) and (d) show results as the lip length is varied. The highest distortional buckling stresses are achieved when the lip length is nearly equal to the flange width ($d/b \sim 1$). Lips longer than this degrade the distortional buckling stress. From the standpoint of distortional buckling (ignoring the detrimental effects of long lips in local buckling modes) edge stiffener lengths should be longer than currently used in practice.

Deep webs lead to low stresses: Comparing the results from the 6 in. deep web to the 12 in. deep web given in Figure 2, the distortional buckling stress decreases approximately by a factor of 2 when the web depth is doubled. Actual decrease in the distortional buckling stress depends on the specific *d* and *b*. Distortional buckling is governed by the rotational stiffness at the web/flange juncture, deeper webs are more flexible and thus provide less rotational stiffness to the web/flange juncture. This results in earlier distortional buckling for deep webs. However, the trend appears approximately linear, as opposed to local buckling which changes as $(t/h)^2$ and thus local buckling stresses decrease at a faster rate with deeper webs.

As Figure 2 shows, the interaction of the flange, web, and lip in determining the distortional buckling stress is complex. Development of simple yet general criteria to incorporate this behavior has not proven successful to date.

Table 1 Summary of Research on Cold-Formed Steel Columns

	Overall	**Distortional Buckling**
1940's and 1950's	• Elastic plate stability formalized • Experimental work begins • Effective width for ultimate strength	• Known phenomena • Too complicated to predict analytically
1960's	• Early design methods formalized • Cold-formed steel material properties • Prediction of overall (global) buckling	• Approximate analytical methods from Aluminum researchers • Folded plate theory for distortional buckling
1970's	• Local and overall interaction • Design methods for unstiffened and edge stiffened elements • Finite Elements	• Observed in experiments, but often intentionally restricted • Elastic buckling criteria not accurate for predicting failure mode
1980's	• Imperfections and residual stresses • Effective width formalized • Finite strip • Distortional buckling problems	• Hand methods for elastic prediction • Experiments with unrestricted distortional buckling performed • Postbuckling reserve discovered
1990 to Present	• Distortional buckling problems • Distortional buckling design • Interaction & column boundary conditions • Generalized Beam Theory	• Hand methods for elastic prediction • Interaction of distortional with other buckling modes examined • Design: column curve or effective width? • Heightened imperfection sensitivity? • Inclusion in Design Standards

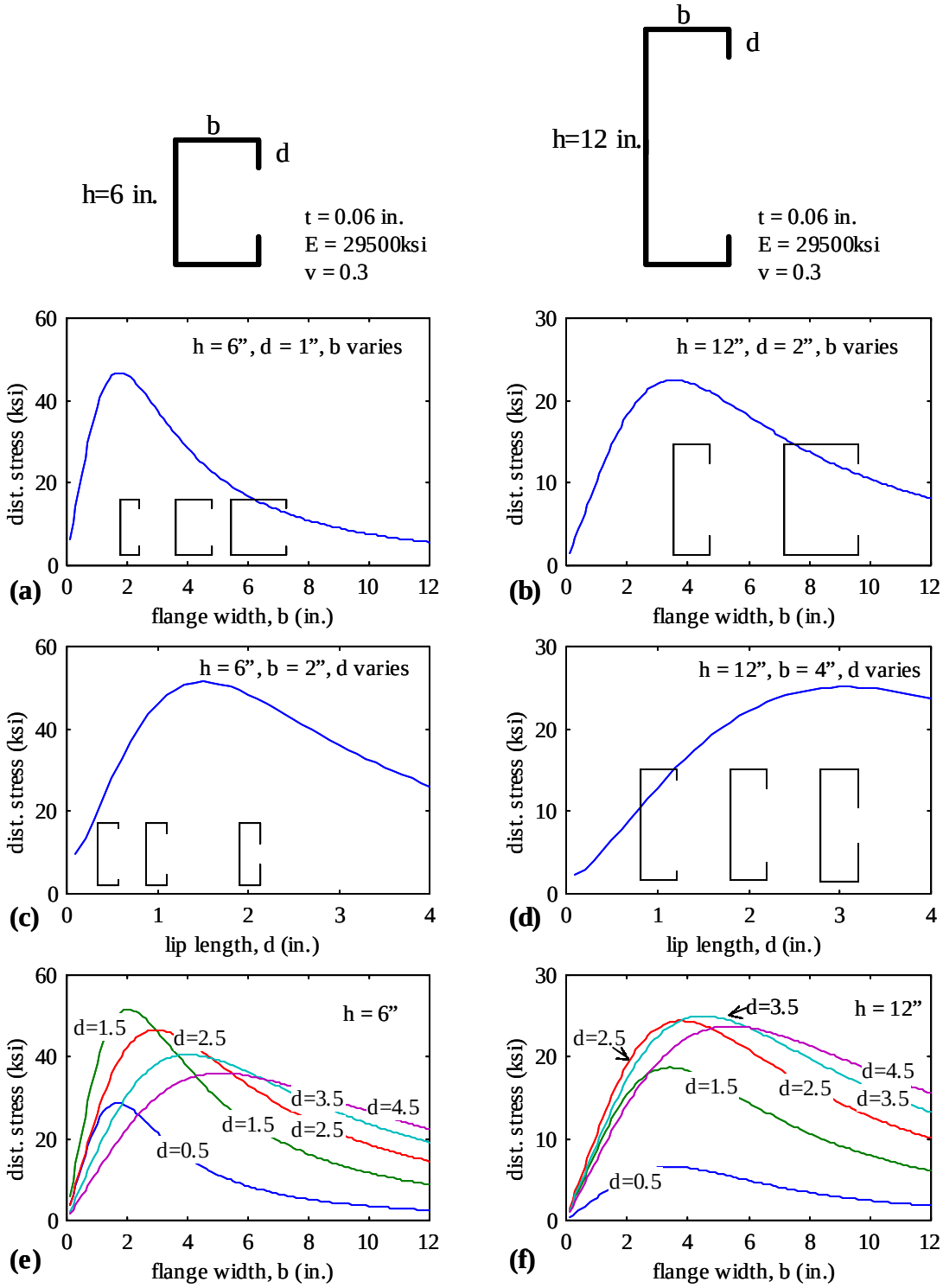

Figure 2 Behavior of Distortional Buckling Stress for Lipped C Columns (a-b) variation with respect to flange width, (c-d) variation with respect to lip length, (e-f) variation with respect to flange width for different lip lengths

What research has already been done for distortional buckling of columns?

Table 1 provides a summary of the history of research in cold-formed steel columns with an emphasis on distortional buckling. A full version of the history of distortional buckling in cold-formed steel column research may be found in Appendix A. Table 1 shows the basic trends in research and design specifications with respect to distortional buckling: notably, the 1990s saw the explicit introduction of distortional buckling into design specifications. Many questions remain to be completely answered: How does distortional buckling interact with other modes? Does the distortional mode exhibit a heightened imperfection sensitivity? How should distortional buckling be incorporated into specifications?

3 Hand Prediction of Column Buckling Modes

Illustrative examples, completed in Mathcad, for the hand prediction of the column buckling modes of Figure 1 are given in Appendix B. The following sections introduce the various prediction methods, and examine the accuracy of the proposed formula versus numerical methods.

3.1 Local Mode

Hand prediction of the local buckling mode may be done in two ways: the traditional, element approach; or a semi-empirical, interaction approach. The element approach is the classic isolated plate solution. For example, employing $k = 4$ for a "stiffened element" assumes it is a simply supported plate in pure compression. Local buckling of the entire member may be predicted by taking the minimum of the connected elements (very conservative approach), alternatively a weighted average may be used, or interaction of elements may be ignored and each element assumed to buckle independently, this is tacitly assumed in the AISI (1996) Specification.

The semi-empirical, interaction approach uses modified plate buckling coefficients (i.e., modified k's) to account for the influence of a single neighboring element. For instance, in Appendix B expressions are given for flange/web local buckling and for flange/lip local buckling. (*Note*: the expression for flange/web local buckling are newly derived for this work.) Local buckling of the entire member may be predicted by taking the minimum of these semi-empirical, interaction equations. A complete example for predictions in the local mode are given in Appendix B.

3.2 Distortional Mode

Closed-form "hand" models fro distortional buckling may be predicted via: current AISI (1996) methods, Lau and Hancock (1987), or Schafer (1997). The AISI (1996) method is based on the work of Desmond (1977) and its development is fully discussed in Appendix A and Schafer (1997). The approaches of Lau and Hancock (called Hancock's approach from hereon) and Schafer's approach are similar. The Hancock and Schafer models are conceptually the same for the flange, but differ in the methods used to treat the web. Schafer's method explicitly approximates the rotational stiffness at the web/flange juncture in the calculation of the distortional buckling stress.

Inaccuracy in the AISI (1996) approach lead to another simplified method for handling distortional buckling. The approach was created by the author – essentially an additional reduction is placed on the AISI k value for high web height to flange width ratios. This reduction approximately accounts for distortional buckling and local buckling interaction. The expression for the reduction, R, is given in the notes of Table 3.

A complete example for predictions in the distortional mode are given in Appendix B.

3.3 Flexural or Flexural-torsional Mode

Hand predictions for x-axis and y-axis flexural buckling as well as approximate hand prediction of flexural-torsional buckling is given in AISI (1996). Calculation of the 'warping' section properties is the only significant complication with these hand methods.

A complete example for predictions in the flexural or flexural-torsional mode are given in Appendix B.

3.4 Accuracy of Hand Predictions for Local and Distortional Buckling

A parametric study of 170 cross-sections is performed in order to assess the accuracy of available hand methods for prediction of local, distortional, and global buckling modes. The geometry of the studied members is shown in

Figure 3, summarized in Table 2 and detailed in Appendix C. A variety of C's and Z's are studied, including all of those listed in the AISI (1996) Design Manual as well as a group of commercially available drywall studs (selected primarily for their relatively high web slenderness). In addition, a group of members covering a large range of element slenderness, originally studied in Schafer (1997), is also included.

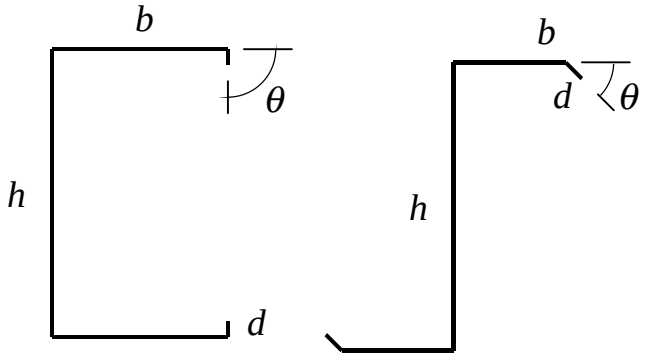

Figure 3 Geometry of Members for Elastic Buckling Study

Table 2 Summary of Member Geometry for Elastic Buckling Study

	h/b		h/t		b/t		d/t		
	max	min	max	min	max	min	max	min	count
Schafer (1997) Members	3.0	1.0	90	30	90	30	15.0	2.5	32
Commercial Drywall Studs	4.6	1.2	318	48	70	39	16.9	9.5	15
AISI Manual C's	7.8	0.9	232	20	66	15	13.8	3.2	73
AISI Manual Z's	4.2	1.7	199	32	55	18	20.3	5.1	50
	7.8	0.9	318	20	90	15	20.3	2.5	170

Overall performance of the prediction methods is shown for local buckling in Figure 4 and distortional buckling in Figure 5. Table 3 presents the summarized numerical information and Appendix C presents the detailed member by member results.

For local buckling prediction Table 3 and Figure 4 show that the semi-empirical interaction model (e.g., *k* calculated as a function of flange width to web width ratios) is clearly more accurate than the element model (each element, web, flange, lip treated separately). This is particularly true for moderate web height to flange width ratios. However, the element model is consistently conservative, and the semi-empirical interaction model may be unconservative for high web height to flange width ratios. This is more than offset by the increased accuracy in the practical range of sections. The semi-empirical interaction model predicts local buckling of the entire member with reasonable accuracy.

For distortional buckling prediction Table 3 and Figure 5 show that the AISI approach is flawed and that both Hancock's and Schafer's method work reasonably well. The existing AISI method is unconservative and inaccurate. Simple modifications proposed with an h/b correction (the R*AISI method) remove the overall unconservative nature of the prediction, but cannot provide the same level of accuracy as the more robust expressions of Hancock's and Schafer's method.

Distortional buckling prediction by Schafer's approach provides a slightly more accurate, but less conservative solution than Hancock's approach. In a finite strip analysis the distortional mode may not always exist as a minimum. In these cases the accuracy of the predictive methods cannot be directly assessed – and statistics for those members are not included in Table 3. However, Appendix C provides a direct member-by-member comparison of the distortional buckling predictions for Schafer's and Hancock's approach. As the web height to flange width ratio (*h/b*) increases (above approximately 4) Hancock's approach often yields a distortional buckling stress of zero. Thus, the method, conservatively indicates no strength exists in these sections. Schafer's approach yields a distortional buckling stress that is at or slightly above the web local buckling stress. Thus in this limit, Schafer's approach converges to the expected solution. This is a result of the more accurate treatment of the web's contribution to the rotational stiffness at the web/flange juncture.

Table 3 Performance of Prediction Methods for Elastic Buckling

		Local		Distortional			
		$\frac{(fcr)_{true}}{(fcr)_{element}}$	$\frac{(fcr)_{true}}{(fcr)_{interact}}$	$\frac{(fcr)_{true}}{(fcr)_{Schafer}}$	$\frac{(fcr)_{true}}{(fcr)_{Hancock}}$	$\frac{(fcr)_{true}}{(fcr)_{AISI}}$	$\frac{(fcr)_{true}}{(fcr)_{R*AISI}}$
All Data	avg.	**1.34**	**1.03**	**0.93**	**0.96**	**0.79**	**1.01**
	st.dev.	0.13	0.06	0.05	0.06	0.33	0.25
	max	1.49	1.15	1.07	1.08	1.45	1.70
	min	0.96	0.78	0.81	0.83	0.18	0.43
	count	149	149	89	89	89	89
Schafer (1997) Members	avg.	**1.16**	**1.02**	**0.92**	**0.96**	**1.09**	**1.16**
	st.dev.	0.15	0.08	0.07	0.06	0.16	0.22
Commercial Drywall Studs	avg.	**1.38**	**1.07**	**0.93**	**1.00**	**0.81**	**1.14**
	st.dev.	0.09	0.05	0.02	0.07	0.26	0.22
AISI Manual C's	avg.	**1.33**	**1.01**	**0.93**	**0.99**	**0.81**	**0.99**
	st.dev.	0.13	0.07	0.05	0.03	0.26	0.19
AISI Manual Z's	avg.	**1.39**	**1.04**	**0.92**	**0.92**	**0.41**	**0.81**
	st.dev.	0.03	0.04	0.03	0.06	0.18	0.24

$(fcr)_{element}$ = minimum local buckling stress of the web, flange and lip
$(fcr)_{interact}$ = minimum local buckling stress using the semi-empirical equations for the web/flange and flange/lip
$(fcr)_{Schafer}$ = distortional buckling stress via Schafer (1997)
$(fcr)_{Hancock}$ = distortional buckling stress via Lau and Hancock (1987)
$(fcr)_{AISI}$ = buckling stress for an edge stiffened element via AISI (1996)
$(fcr)_{R*AISI}$ = reduced buckling stress for an edge stiffened element, R=0.65/(h/b-1), h/b>1.65

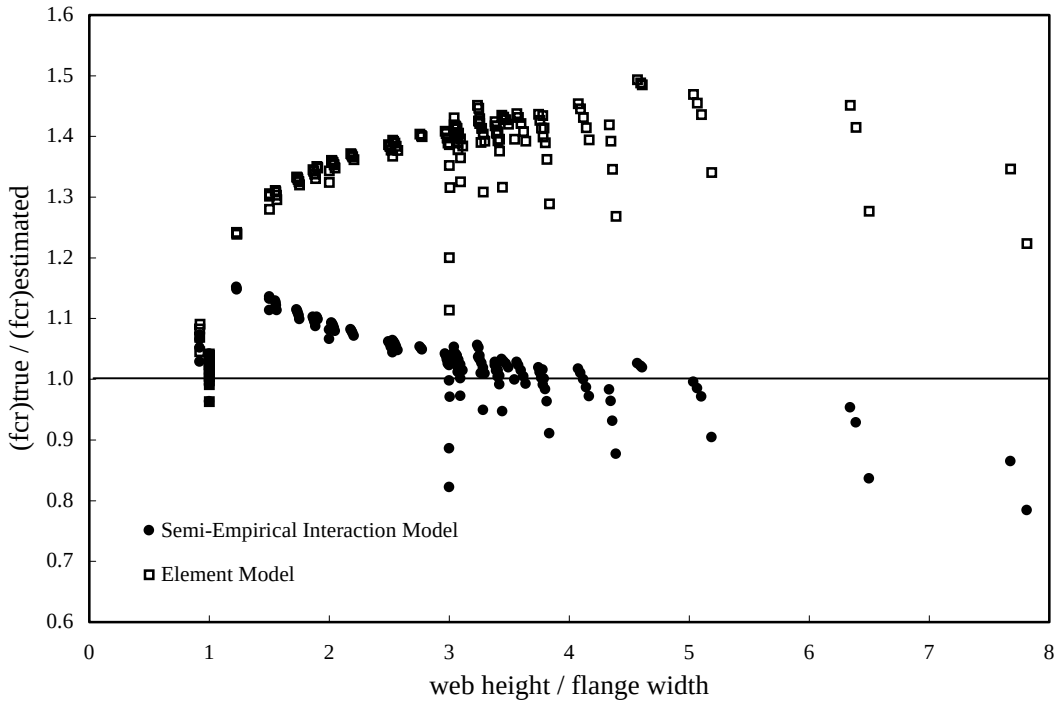

Figure 4 Performance of Local Buckling Prediction Methods

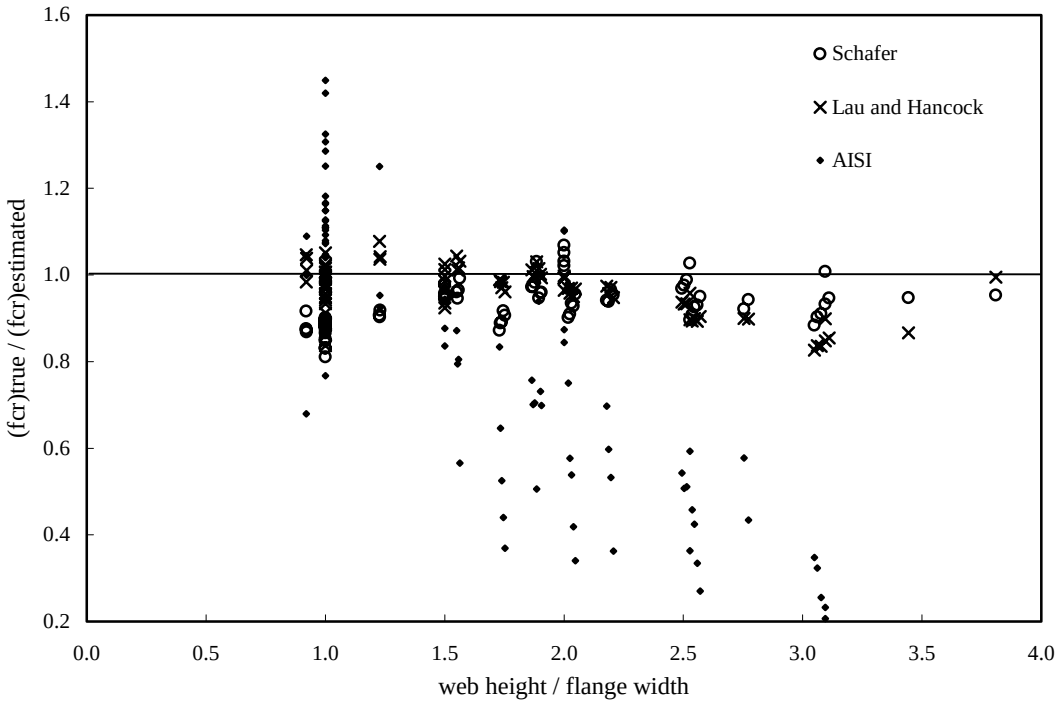

Figure 5 Performance of Distortional Buckling Prediction Methods

4 Understanding When the Distortional Mode is Prevalent

The AISI (1996) Specification does not explicitly treat distortional buckling as a separate mode of failure. Further, as the previous section indicated, existing AISI equations for predicting distortional buckling are inadequate for a large variety of common members. For columns, how important is this failure of the AISI Specification to predict distortional buckling? To answer this, and to provide more overall insight into distortional buckling we must answer the question: When is the distortional mode prevalent?

For lipped C's, the introduction, specifically Figure 2 and the related discussion, provide general guidance to address the issue of when the distortional mode is prevalent. Distortional buckling stresses are low when the flanges are very narrow (flange width less than approximately 1/6 the web height) or very wide (flange width greater than approximately 3/4 the web height). Members with narrow flanges are generally controlled by local buckling even though distortional buckling stresses are low because the web is much more slender than the flange and buckles locally first. If intermediate stiffeners are added in the web then members with narrow flanges are likely to suffer distortional failures.

Members with wide flanges (shapes approaching square) tend to have more problems with distortional buckling because as the shape approaches the square geometry distortional buckling stresses decrease while local buckling stresses increase. Eventually this leads to sections which are generally controlled by distortional limits.The distortional mode is not prevalent in members with long lips. Even though the distortional buckling stress eventually decreases for exceedingly long lips (see Figure 2 c and d) – the reductions in local buckling are more pronounced. Long lips retard the distortional mode and trigger the local mode.

Numerical examples follow to further reinforce these general concepts. Consider the members introduced in Table 2 and detailed in Appendix C. For all 170 of these members the buckling mode for the minimum elastic buckling stress (local vs. distortional) is determined via finite strip, and plotted against the web height (h) to flange width (b) ratio, as shown in Figure 6. For the vast majority of these members local buckling is the dominant mode of failure. In fact, for $h/b > 2$ essentially all of the members have a local buckling stress lower than distortional buckling. The exception is a couple of Z sections which have short sloping stiffeners, such a flange has little rotational stiffness to provide at the web/flange juncture.

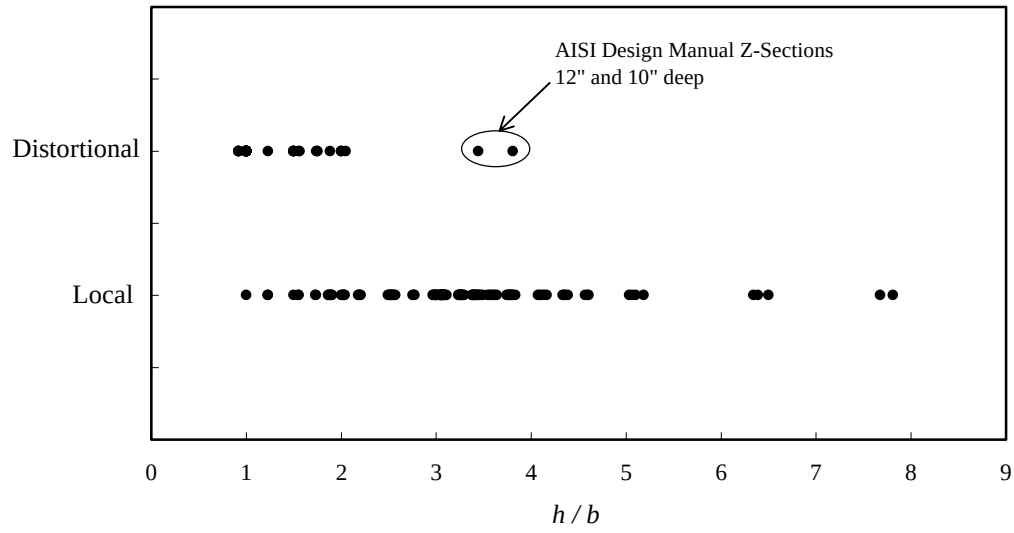

Figure 6 Minimum Elastic Buckling Mode for Studied Sections

4.1 In a Typical Lipped Channel Column

To better understand how local and distortional buckling are competing the studied members are broken into their specific cross-section type. In Figure 7 the buckling stress (via finite strip) in the local and distortional mode for both the AISI Lipped C sections (from the design manual) and a set of commercially available drywall studs are examined. Local buckling primarily follows a curve dominated by the web slenderness (h/t). For the majority of

these members the web is markedly more slender than the compression flange. The distortional buckling results exhibit a greater scatter than local buckling but for typical C sections members with $h/t < 100$ appear most prone to distortional buckling.

The points with a buckling stress of "zero" represent cases in which the finite strip analysis does not have a minimum in that mode. For instance, analysis of the members with high web slenderness typically only revealed a local buckling minimum, this is evidenced by the large number of distortional points along the "zero" line in the region of high web slenderness. In these situations investigation of higher modes will reveal the distortional buckling minimums; however this was not done in this case.

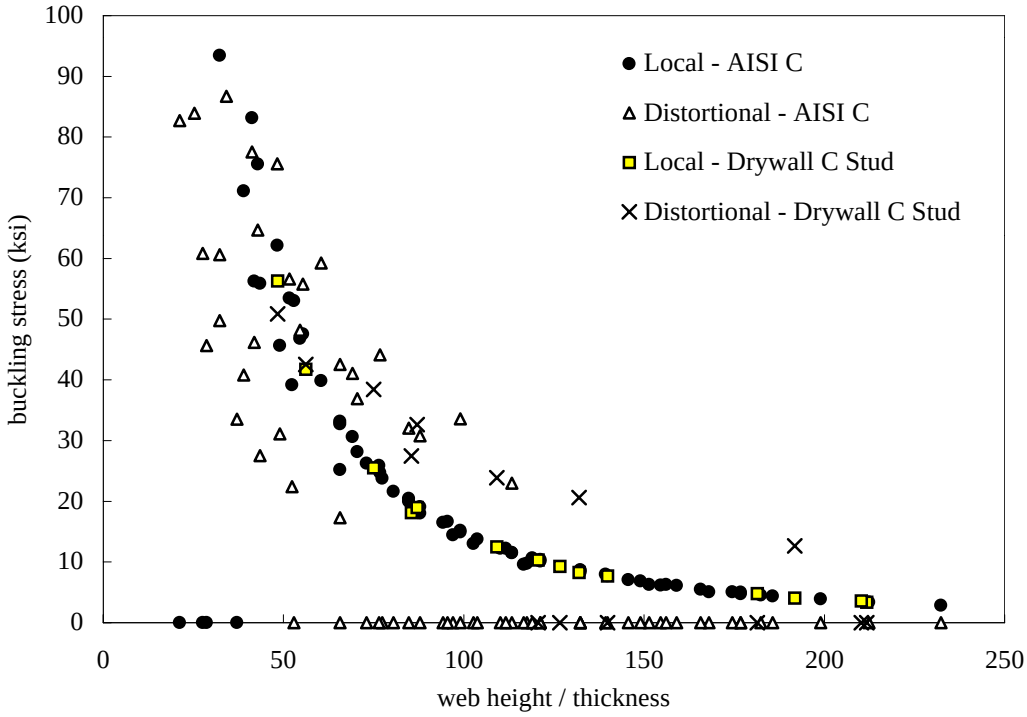

Figure 7 Local and Distortional Buckling of Lipped C's

4.2 In a Z section Column

A similar analysis, as conducted in the previous section, is performed for the Z sections in the AISI design manual, as shown in Figure 8. Local buckling of the entire member is again dominated by the web slenderness. As before, this is due to the fact that all of these members have web depths much greater than the flange width. Distortional buckling and local buckling occur at similar buckling stresses for a large variety of members. At first glance distortional buckling appears to follow the web slenderness closely as well, however closer inspection at h/t approximately 60 and 80 reveal that this is not always the case. Further, the sections used in the AISI Design Manual have little variation in the stiffener selection. Greater variation in the stiffener length, as done in Schafer (1997) reveals a scatter more like that of Figure 7. For standard Z sections distortional buckling appears most prevalent in the members with $h/t < 100$.

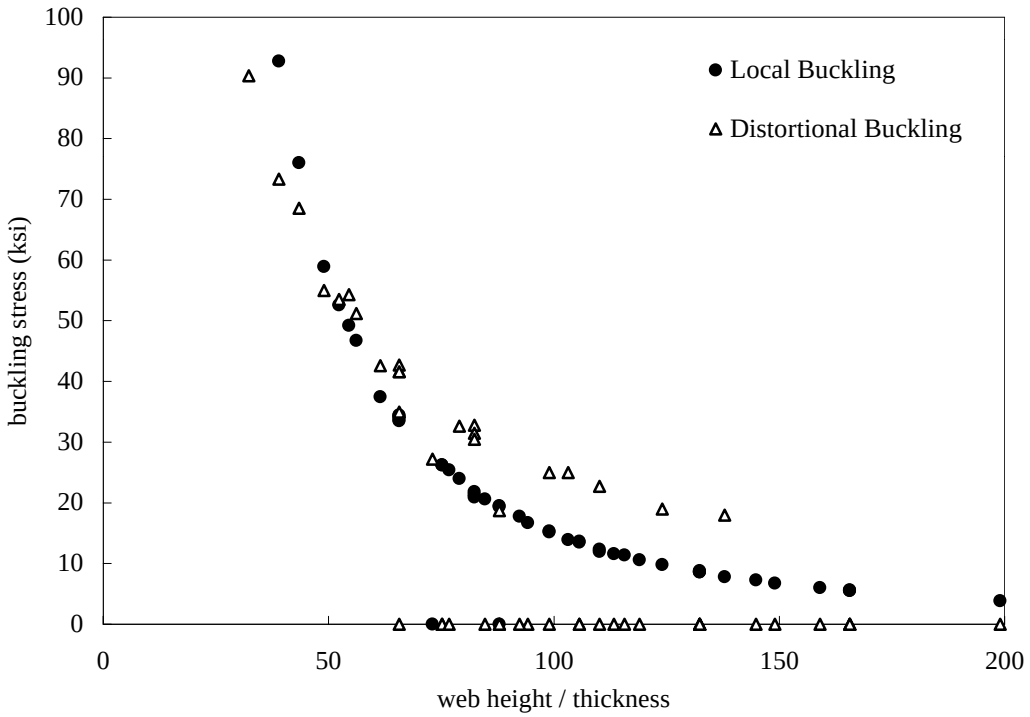

Figure 8 Local and Distortional Buckling of Z's

4.3 In Optimized Shapes

In typical Lipped C and Z shaped members the local mode is most prevalent. This is due to the slender nature of the web. An obvious way to eliminate this mode is to provide a longitudinal stiffener in the web and thus increase the local buckling stress. This idea has been experimentally studied in compression members by Thomasson (1978) and Kwon and Hancock (1992).

A parametric study which modifies the lipped C sections in the AISI Design Manual, as shown in Figure 9, is conducted here. A web stiffener with the same horizontal and vertical dimensions as the existing lip stiffener is introduced into the web. The resulting local and distortional modes are shown in Figure 10. The numerical results, depicted in Figure 11, indicate that while the stiffener markedly increases the local buckling stress now distortional buckling is not only prevalent, but is a far more dominant mode of behavior than the local mode.

In Figure 11 the curve for local buckling without a stiffener is also shown. For $h/t > 60$ there is an improvement in the elastic buckling stress of all the members; the stiffener provides a benefit. However, the cost is that the mode of failure is now a distortional one (Figure 10(b)) and thus significantly different than local buckling without the intermediate stiffener. Experimental and analytical evidence indicates that the distortional mode is more imperfection sensitive and has a reduced post-buckling capacity. From an elastic buckling standpoint the improvement due to the intermediate stiffener is clear; however it is not clear what the exact ultimate benefit is.

Optimization of the cross-section through adding additional folds may greatly benefit the ultimate strength, but also often directly leads to a need to more prominently consider the distortional mode.

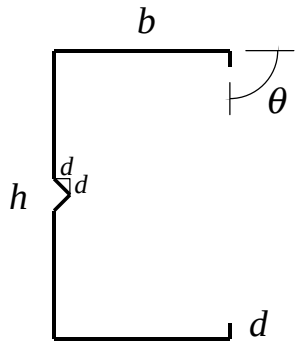

Figure 9 Geometry of Lipped C's with a Web Stiffener

(a) Local Buckling (b) Distortional Buckling

Figure 10 Local and Distortional Buckling of Lipped C with a Web Stiffener

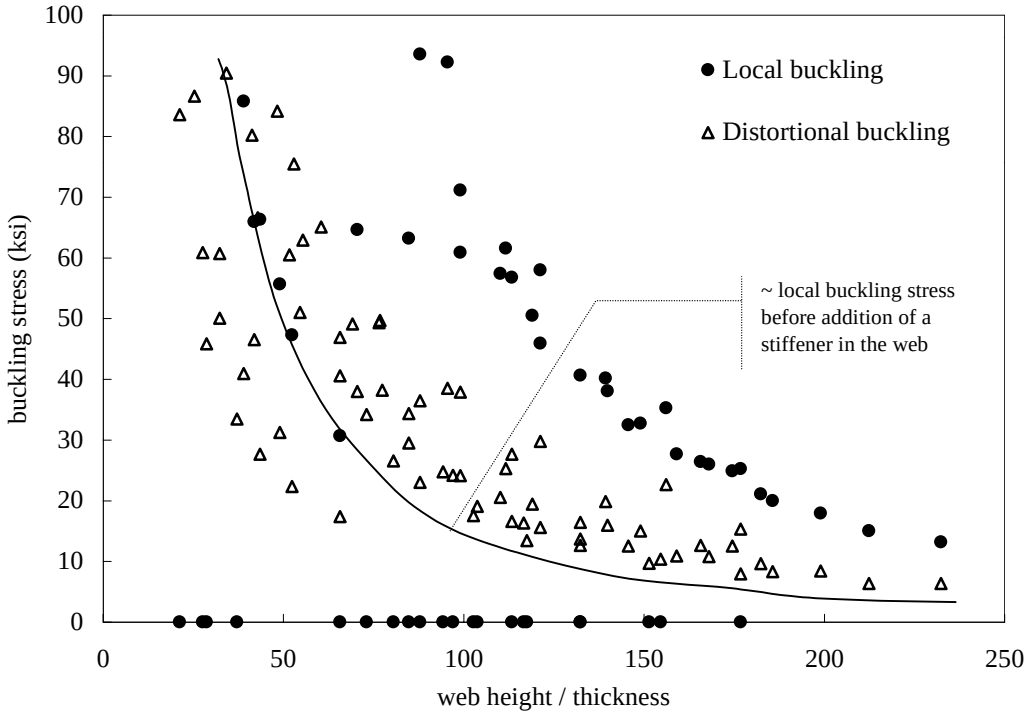

Figure 11 Local and Distortional Buckling of Lipped C's with a web stiffener

5 Ultimate Strength in the Distortional Mode

5.1 Numerical Studies

Finite element analysis of the ultimate strength of cold-formed steel elements and members was investigated in Schafer (1997). Examination of the ultimate strength of isolated edge stiffened elements with a variety of geometric dimensions demonstrated that:

- distortional failures have lower post-buckling capacity than local buckling modes of failure, see Figure 12,
- distortional buckling may control failure even when the elastic distortional buckling stress (load) is higher than the elastic local buckling stress (load), see Figure 13, and
- distortional failures have higher imperfection sensitivity, see Figure 14.

As a result of these facts the distortional mode has a lower strength curve than local buckling (i.e., Winter's curve is unconservative), lower ϕ factors may be needed for strength prediction in the distortional mode, and since elastic buckling is not a direct indicator of the final failure mode - complications arise in the prediction of the actual failure mode.

Numerical analysis of a series of lipped channel columns demonstrate that the ultimate strength of columns which fail in the distortional buckling mode can be predicted through knowledge of the elastic distortional buckling stress (load) of the column. The geometry of the studied columns is presented in Figure 15 and Table 4. The ultimate strength of the columns is shown in Figure 16.

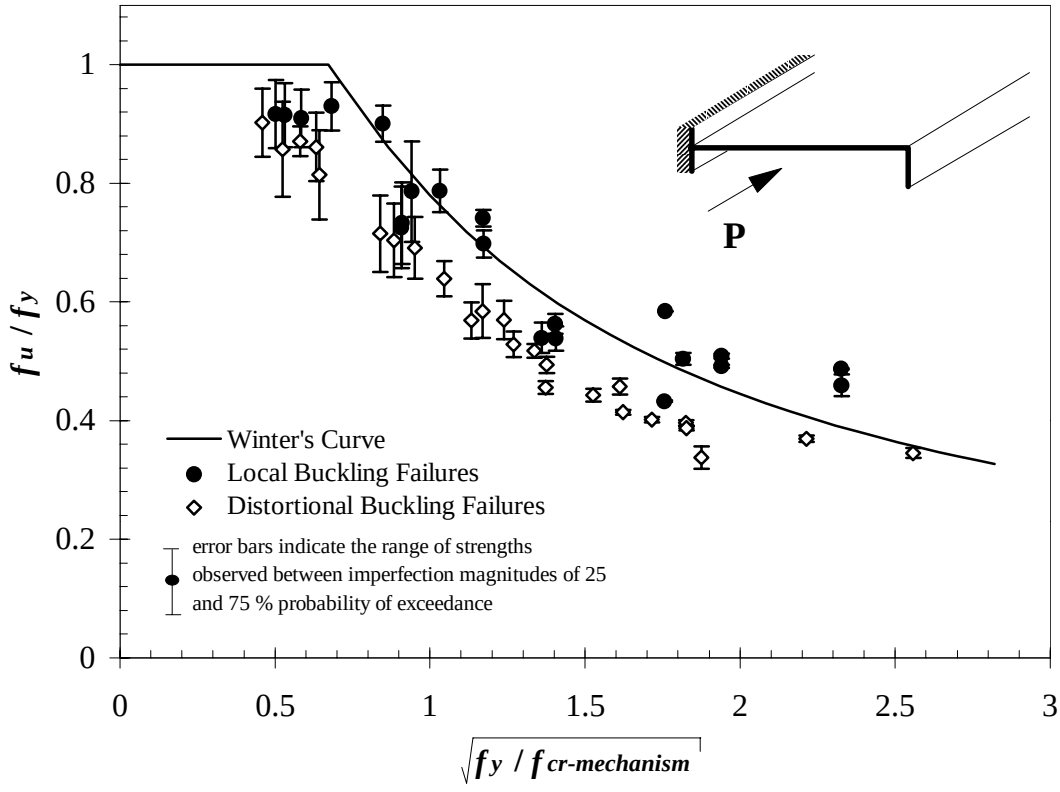

Figure 12 Lower post-buckling capacity in distortional mode: finite element analysis of edge stiffened element

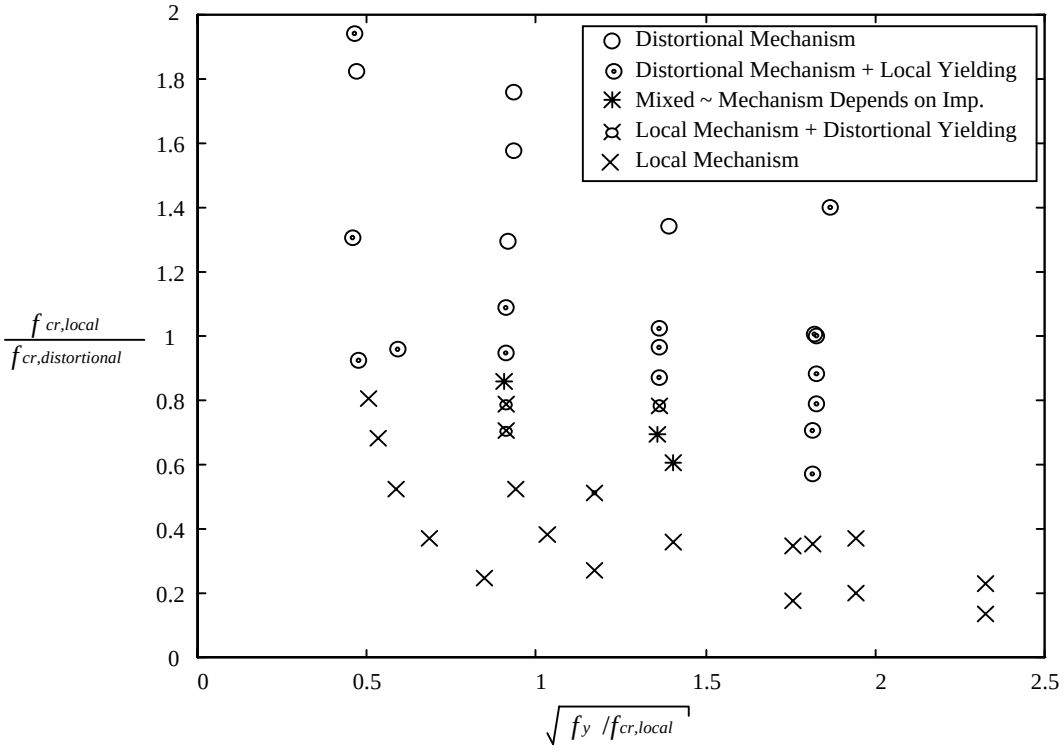

Figure 13 Minimum elastic buckling stress does not predict failure mode: finite element analysis of edge stiffened element

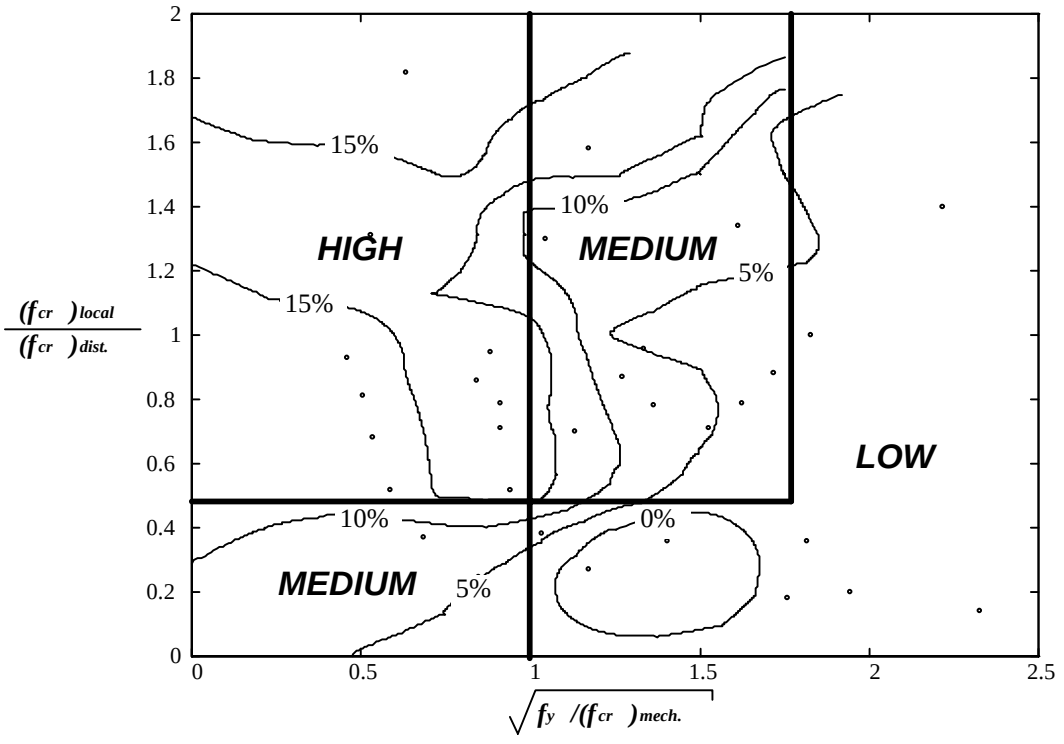

Figure 14 Heightened imperfection sensitivity in distortional failures: finite element analysis of edge stiffened element

Table 4 Geometry of members in pure compression studied via finite element analysis

H	*B*	*D*	θ
30	30	2.5,5	45,90
60	30	2.5,5	45,90
	60	2.5,5,10	45,90
90	30	2.5,5	45,90
	60	2.5,5,10	45,90
	90	2.5,5,10,15	45,90

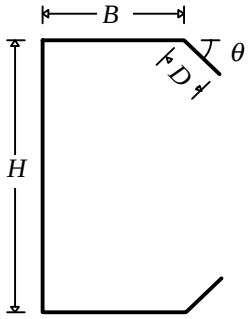

Figure 15 Geometry of members in pure compression studied via finite element analysis

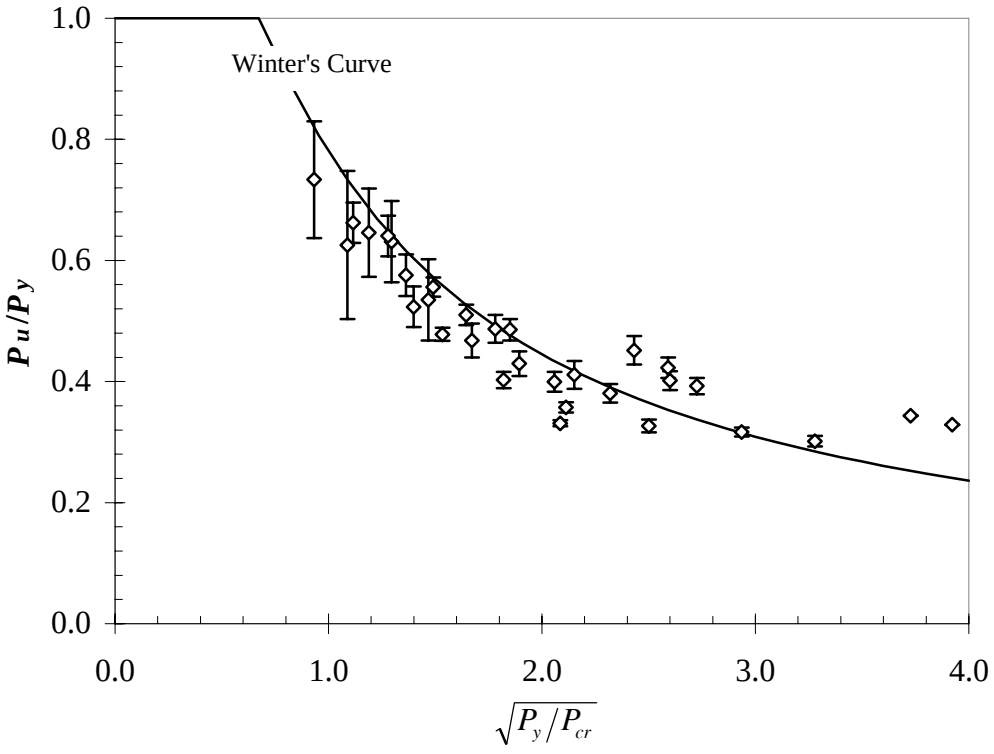

Figure 16 Ultimate strength of columns in pure compression failing in distortional buckling, studied via finite element analysis (Note, error bars indicate the range of strength between imperfection magnitudes of 25 and 75 % probability of exceedance.)

5.2 Experimental Data

The most convincing experimental evidence for the prediction of the strength of cold-formed steel columns failing in the distortional mode is derived from the work conducted at the University of Sydney: Lau and Hancock (1987), Kwon and Hancock (1992) as summarized in Hancock et al. (1994). Compression tests were conducted on: (a) lipped channels, (b) rack column uprights, (c) rack column uprights with additional outward edge stiffeners, (d) hats, and (e) lipped channels with a web stiffener as shown in Figure 17. The ultimate strength is reported in Figure 18.

The expression fit to the distortional buckling failures of Figure 18 is known as the Modified Winter Curve or "Hancock's curve" and may be expressed as:

$$\frac{P_n}{P_y} = \left(1 - 0.25\left(\frac{P_{crd}}{P_y}\right)^{.6}\right)\left(\frac{P_{crd}}{P_y}\right)^{.6} \quad \text{where } \sqrt{\frac{P_y}{P_{crd}}} > 0.561, \text{ otherwise } \frac{P_n}{P_y} = 1 \ .$$

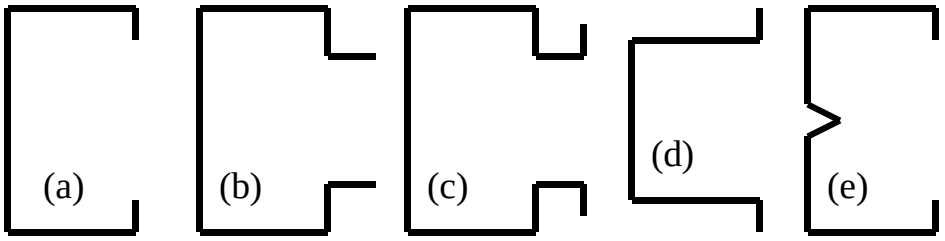

Figure 17 Geometry of columns studied at U. of Sydney

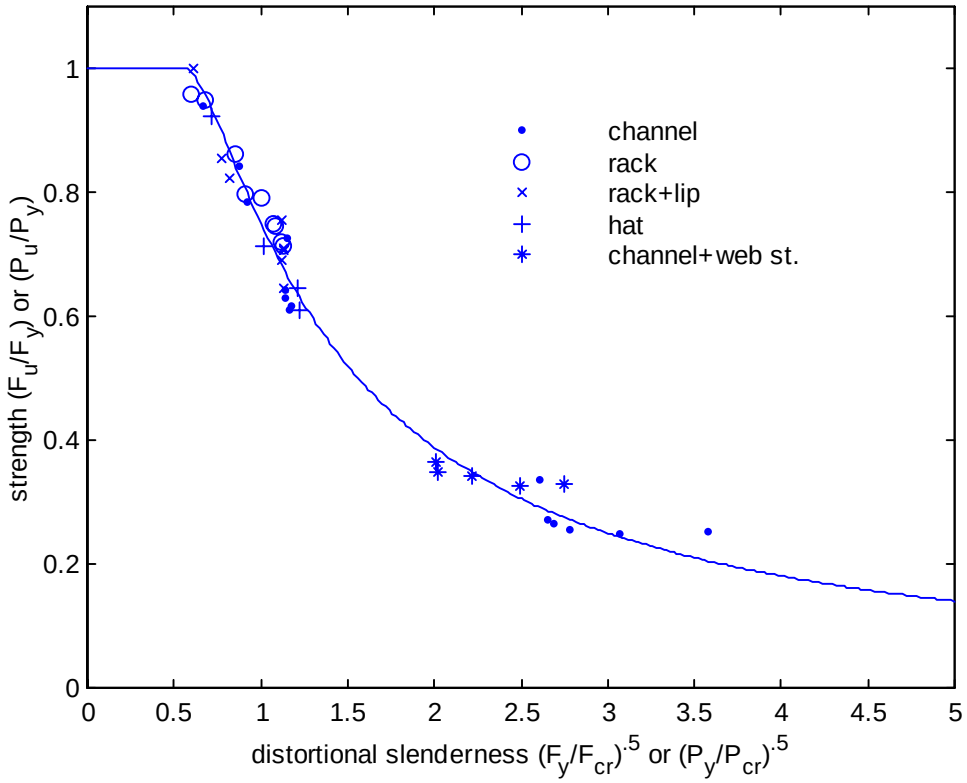

Figure 18 Ultimate strength of columns failing in distortional buckling (U. of Sydney tests)

where:

P_n is the nominal capacity
P_y is the squash load ($A_g f_y$)
P_{crd} is the critical elastic distortional buckling load

Figure 18 provides strong evidence that *if the failure is known to occur in the distortional mode*, then the elastic distortional buckling load (stress) may be used to predict the ultimate strength. This fact appears true for a variety of different cross-sections. Note that the current AISI (1996) Specification has no rules which would govern the strength of many of the investigated members.

The prevalence of the distortional failure mode in these tests is increased due to the use of high strength steel. For two members with identical geometry, but different yield stress, a high strength steel member will have the greater slenderness - as Figure 13 shows, as slenderness increases the prevalence of the distortional mode increases.

Recent additional work on rack columns such as Figure 17(c), but with perforations, have also investigated distortional buckling (Baldassino and Hancock 1999). Based on comparisons to hand methods for the prediction of distortional buckling, they found that use of the minimum net area for computation of the distortional buckling strength, was unconservative – instead they used an effective area which accounts for local buckling. Based on this result they concluded that local and distortional buckling may interact in perforated rack columns.

6 Design Methods

Consider the general design problem of a cold-formed steel column. Identification of the possible limit states for the column, with consideration for interaction between modes creates a large variety of different possible failure mechanisms:

- local,
- distortional,
- long column Euler buckling,
- local interaction with distortional,
- local interaction with Euler,
- distortional interaction with Euler, and
- all three basic modes: local, distortional, Euler interacting.

Currently, the AISI (1996) Specification uses an effective width approach to accommodate local buckling. In the AISI approach, interaction with Euler buckling is handled by limiting the stress in the effective width determination to the nominal column buckling stress (F_n). Distortional buckling is not directly treated in the AISI approach, and interaction with distortional buckling and other modes is not considered.

Table 6 presents a general outline to the various possibilities of the design of cold-formed steel columns. Each limit state is identified. Methods for examining elastic buckling and the ultimate strength are identified. The methods presented in Table 6 summarize current “element” approaches to the design of cold-formed steel as well as the member level “direct strength” approaches that have been recently investigated for cold-formed steel bending members (Schafer and Peköz 1998). All new design methods are investigated for various combinations presented in Table 6.

Eleven different design methods are selected for investigation, as detailed in Table 5. Four basic types of design methods are considered:

A. the current AISI approach and small variations, e.g. adding a distortional check,

B. methods which consider local interaction with long column buckling, but ignore any distortional interactions,

C. methods which consider local or distortional interaction with long column buckling, and

D. methods which consider local and distortional interaction as well as local or distortional interaction with long column buckling.

In each of types B through D, three types of design methods are considered.

1. "Element" type solutions, where local buckling is considered by finding the effective width of each isolated element and using Winter's curve to determine the strength (similar to AISI in concept, but local buckling is always assumed, for instance the flange of an edge stiffened element always uses k = 4, not a modified k); distortional buckling is considered as either a separate failure mode (member level solution) or compared versus the elastic local buckling stress (element level solution).

2. "Member" solutions where a local buckling stress (load) is determined for the member as a whole and a local buckling strength is found by using an alternative strength curve (i.e., $P_n/P_y=(1-0.15(P_{crL}/P_y)^{0.4})(P_{crL}/P_y)^{0.4}$). Distortional buckling stress (load) is also determined for the member as a whole and a different strength curve (Hancock's curve) is used. In this solution hand methods are used for all calculations.

3. Identical to, 2, except finite strip solutions are used for the buckling stress (load) in local and distortional buckling instead of hand methods.

Appendix D provides a design example for each of the 11 separate methods.

Table 5 Key to investigated design methods (indices refers to methods outlined in Table 6)

Label	(L)ocal	(D)istortional	(E)uler	L+D	L+E	D+E
A1	1.a.i.a.i	-	3.a.i.a.i	-	5.a.i.a	-
A2	1.a.i.a.i	2.b.i.b.ii	3.a.i.a.i	-	5.a.i.a	-
B1	1.a.ii.a.i	2.b.i.b.ii	3.a.i.a.i	-	5.a.ii.a	-
B2	1.b.i.b.ii	2.b.i.b.ii	3.a.i.a.i	-	5.b.i.b(1.b.i)	-
B3	1.b.ii.b.ii	2.b.ii.b.ii	3.a.i.a.i	-	5.b.i.b(1.b.ii)	-
C1	1.a.ii.a.i	2.a.ii.a.ii	3.a.i.a.i	-	5.a.ii.a	6.b.i.b(2.b.i)
C2	1.b.i.b.ii	2.b.i.b.ii	3.a.i.a.i	-	5.b.i.b(1.b.i)	6.b.i.b(2.b.i)
C3	1.b.ii.b.ii	2.b.ii.b.ii	3.a.i.a.i	-	5.b.i.b(1.b.ii)	6.b.i.b(2.b.ii)
D1	1.a.ii.a.i	2.a.ii.a.ii	3.a.i.a.i	4.a.ii.a(2.a.ii)	5.a.ii.a	6.b.i.b(2.b.i)
D2	1.b.i.b.ii	2.b.i.b.ii	3.a.i.a.i	4.b.i.b(1.b.i,2.b.i)	5.b.i.b(1.b.i)	6.b.i.b(2.b.i)
D3	1.b.ii.b.ii	2.b.ii.b.ii	3.a.i.a.i	4.b.i.b(1.b.ii,2.b.ii)	5.b.i.b(1.b.ii)	6.b.i.b(2.b.ii)

For example, A1=AISI method, local, Euler, and local+Euler interaction is considered; local buckling strength is completed by the method outlined in 1.a.i.a.i in Table 3, Euler buckling strength is completed by the method outlined in 3.a.i.a.i in Table 3, and Local and Euler interaction is completed by 5.a.i.a in Table 3.

Table 6 Summary of Design Method Possibilities for Cold-Formed Steel Column

COLD-FORMED STEEL COLUMNS BASIC LIMIT STATES AND STRENGTH DETERMINATION		
Failure Mode/Mechanism	**Elastic Buckling Calculation**	**Ultimate Strength determination**
1. Local (considered in design)	a. element by element (f_{crL}) i. AISI expressions ii. local only, "k=4" solutions	a. effective width determimed using f_{crL} and f_y i. Winter's curve: $b_{eff}=\rho b$, $\rho=(1-0.22(f_{crL}/f_y)^{0.5})(f_{crL}/f_y)^{0.5}$ ii. alternative strength curves
	b. member (P_{crL}) i. hand solutions ii. numerical (finite strip)	b. strength directly determined using P_{crL} and P_y i. Winter's curve: $P_{ult}=\rho P_y$, $\rho=(1-0.22(P_{crL}/P_y)^{0.5})(P_{crL}/P_y)^{0.5}$ ii. alternative curves, e.g.: $\rho=(1-0.15(P_{crL}/P_y)^{0.4})(P_{crL}/P_y)^{0.4}$
	c. back calc. from stub column test	c. from stub colun test
2. Distortional (mostly ignored in design)	a. element by element (f_{crD}) i. AISI expressions approx. this ii. hand solutions (Hancock or Schafer) iii. numerical finite strip	a. effective width determined using f_{crD} and f_y i. Winter's curve: $b_{eff}=\rho b$, $\rho=(1-0.22(f_{crD}/f_y)^{0.5})(f_{crD}/f_y)^{0.5}$ ii. Winter's curve with f_{crD} lowered to $R_d f_{crD}$ iii. Hancock's curve: $\rho=(1-0.25(f_{crD}/f_y)^{0.6})(f_{crD}/f_y)^{0.6}$ iv. alternative strength curves
	b. member (P_{crD}) i. hand solutions (Hancock or Schafer) ii. numerical (finite strip)	b. strength directly determined using P_{crD} and P_y i. Winter's curve with P_{crD} lowered to $R_d P_{crD}$ ii. Hancock's curve: $\rho=(1-0.25(P_{crD}/P_y)^{0.6})(P_{crD}/P_y)^{0.6}$ iii. alternative strength curves
3. Long (Euler) (considered in design)	a. member (f_{crE} or P_{crE}) i. AISI expressions ii. numerical (finite strip)	a. strength using f_{crE} and f_y or P_{crE} and P_y i. AISI column curve, e.g.: $f_{nE}=0.877 f_{crE}$ or $P_n=0.877 P_{crE}$
4. Local+Distortional (mostly ignored in design)	a. element by element (f_{crL} and f_{crD}) i. "AISI" - f_{crL} by 1.a.i. and f_{crD} by 2.a.i. ii. f_{crL} by 1.a.ii and f_{crD} by 2.a.ii or iii	a. effective width with local post-buckling limited by f_{nD} (i.e. replace f_y with f_{nD} in 1.a-a) f_{nD} is inelastic distortional stress determine f_{nD} from $f_{nD}=\rho f_y$ and an expression in 2.a.-a.
	b. member (P_{crL} and P_{crD}) i. P_{crL} by 1.b. or 1.c and P_{crD} by 2.b.	b. direct strength with local post-buckling limited by P_{nD} (i.e. replace P_y with P_{nD} in 1.b-b) P_{nD} is inelastic distortional load determine P_{nD} from $P_{nD}=\rho P_y$ and an expression in 2.b.-b.
5. Local+Long (considered in design)	a. element by element (f_{crL} and f_{crE}) i. AISI - f_{crL} by 1.a.i. and f_{crE} by 3.a. ii. f_{crL} by 1.a.ii and f_{crE} by 3.a.	a. effective width with local post-buckling limited by f_{nE} (i.e. replace f_y with f_{nE} in 1.a-a) f_{nE} is inelastic Euler buckling stress determine f_{nE} from expression in 3.a.-a.
	b. member (P_{crL} and P_{crE}) i. P_{crL} by 1.b. or 1.c and P_{crE} by 3.a.	b. direct strength with local post-buckling limited by P_{nE} (i.e. replace P_y with P_{nE} in 1.b-b) P_{nE} is inelastic Euler buckling load determine P_{nE} from expression in 3.a.-a.
6. Distortional+Long (mostly ignored in design)	a. element by element (f_{crD} and f_{crE}) i. f_{crD} by 2.a.ii or iii and f_{crE} by 3.a.	a. effective width with distortional post-buckling limited by f_{nE} (i.e. replace f_y with f_{nE} in 2.a-a) f_{nE} is inelastic Euler buckling stress determine f_{nE} from expression in 3.a.-a.
	b. member (P_{crD} and P_{crE}) i. P_{crD} by 2.b. and P_{crE} by 3.a.	b. direct strength with distortional post-buckling limited by P_{nE} (i.e. replace P_y with P_{nE} in 1.b-b) P_{nE} is inelastic Euler buckling load determine P_{nE} from expression in 3.a.-a.
7. Local+Dist.+Long (ignored)	Interaction of all 3 modes is currently ignored. The inelastic buckling stress would have to consider multiple modes; e.g. local post-buckling limited by inelastic buckling stress for distortional and long column interaction.	

7 Experimental Data: Lipped Channels and Z's

Unlike the experimental data conducted at the University of Sydney, the majority of experiments do not identify the failure mode of the column. Thus, distortional buckling must be examined within the context of general strength prediction of cold-formed steel columns, rather than as an isolated event.

7.1 Lipped Channels

Experimental data on cold-formed lipped C columns was collected from Mulligan (1983), Thomasson (1978), and Loughlan (1979) as summarized in Peköz (1987). Additional tests on lipped C's were also collected from Miller and Pekoz (1994). Only unperforated sections, with 90 degree edge stiffeners, tested in a pin-pin configuration were selected for this study. The geometry of the tested sections is summarized in Table 7, where *h*, *b*, and *d* are centerline dimensions defined in Figure 15, and $\theta = 90$.

The experimental data on lipped channels represents a wide variety of sections; in particular, slender webs, slender flanges, and relatively long lips are all tested. However, in the vast majority of the sections (95 out of 102) *h/b* is greater than 1.6 – only in 4 specimens is h/b less than 1. Thus, in essentially all of the tested sections the web is significantly more slender than the flange - in this case, local buckling is more dominant than the distortional mode of behavior (given a reasonable choice of lip length). Thus, this data set provides an examination of columns with *h/b* greater than 1.6, but for typical rack columns or other columns approaching a more square configuration the available data is incomplete. The behavior of rack columns and those sections approaching a more square configuration motivated the original testing on distortional buckling at the University of Sydney (see Figure 18).

Table 7 Geometry of experimental data on lipped channel columns

	h/b		*h/t*		*b/t*		*d/t*		
	max	min	max	min	max	min	max	min	count
Loughlan (1979)	5.0	1.6	322	91	80	30	33	11	33
Miller and Pekoz (1994)	4.6	2.5	170	46	38	18	8	5	19
Mulligan (1983)	2.9	1.0	207	93	93	64	16	14	13
Mulligan (1983) Stub Columns	3.9	0.7	353	65	100	33	22	7	24
Thomasson (1978)	3.0	3.0	472	207	159	69	32	14	13
	5.0	0.7	472	46	159	18	33	5	102

7.2 Z-Sections

A set of experiments on Z-section columns is compiled in Polyzois and Charnvarnichborikarn (1993). The geometry is shown in Figure 19 and summarized in Table 8. The tested sections have right angle (θ=90) edge stiffeners rather than the typical 50° sloping lip stiffeners. Work on elastic buckling with sloping edge stiffeners indicate distortional buckling is more prevalent in members with sloping lips vs. right angle lips (Schafer 1997). The *h*/*b* ratios are similar to those of the lipped channel columns – and thus this data suffers from the same limitations cited above for the lipped channel columns.

The researchers specifically investigated the case of small, or no edge stiffening lip at all. For small edge stiffeners distortional buckling may control the failure mode, even when the *h*/*b* ratio is high (i.e., even when the web slenderness is significantly greater than the flange slenderness.). The experiments show that as the edge stiffener length is increased the strength increases until a limiting maximum is reached. This basic behavior is the motivation for the current AISI Specification rules developed based on tests by Desmond (1977). Unlike the data on lipped channels, this experimental database was not used to calibrate the existing AISI Specification rules for columns; therefore it provides an independent set of data for examination of current procedures.

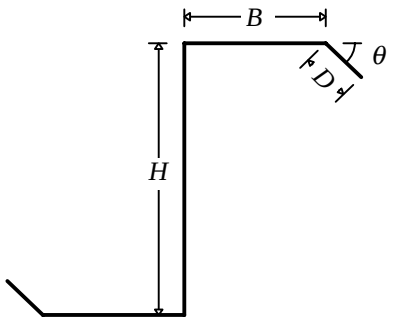

Figure 19 Geometry of Z section columns (θ=90 in selected data)

Table 8 Geometry of experimental data on Z section columns

	h/b		*h/t*		*b/t*		*d/t*		
	max	min	max	min	max	min	max	min	count
Polyzois and Charnvarnichborikarn (1993)	2.7	1.5	137	76	56	30	36	0	85

8 Performance of Design Methods for Lipped C and Z Sections

Using the collected experimental data eleven different design methods were selected for investigation, as detailed in Table 5 and shown in Appendix D. Four basic types of design methods are considered:

A. the current AISI approach and small variations, e.g. adding a distortional check,

B. methods which consider local interaction with long column buckling, but ignore any distortional interactions,

C. methods which consider local or distortional interaction with long column buckling, and

D. methods which consider local and distortional interaction as well as local or distortional interaction with long column buckling.

In each of types B through D, three types of design methods are considered.

1. "Element" type solutions, where local buckling is considered by finding the effective width of each isolated element and using Winter's curve to determine the strength (similar to AISI in concept, but local buckling is always assumed, for instance the flange of an edge stiffened element always uses k = 4, not a modified k); distortional buckling is considered as either a separate failure mode (member level solution) or compared versus the elastic local buckling stress (element level solution).

2. "Member" solutions where a local buckling stress (load) is determined for the member as a whole and a local buckling strength is found by using an alternative strength curve (i.e., $P_n/P_y=(1-0.15(P_{crL}/P_y)^{0.4})(P_{crL}/P_y)^{0.4}$). Distortional buckling stress (load) is also determined for the member as a whole and a different strength curve (Hancock's curve) is used. In this solution hand methods are used for all calculations.

3. Identical to, 2, except finite strip solutions are used for the buckling stress (load) in local and distortional buckling instead of hand methods.

8.1 Overall – for Lipped C and Z Sections

For the investigated design methods, the mean test to predicted ratios for tests on lipped C and Z sections is given in Table 9; in addition the mean test to predicted ratio broken down by limit state is given in Table 10. Methods A1 (current AISI Specification) through C3 all perform reasonably well. However, the "D" methods perform poorly

(overly conservative). This indicates that in the available test data, local and distortional interaction is not significant.

Distortional buckling is not a prevalent failure mode in the experimental data set on lipped C's. Based on the prediction of method C3 (a Direct Strength method with different strength curves for local and distortional modes), only 18 of 102 experiments are identified as having lower strength in the distortional mode than the local mode. This is consistent with the geometry of these members which have wide webs and reasonably sized flanges and lip stiffeners.

Distortional buckling is more prevalent in the experimental data set on Z sections. Based on method C3, 25 of 85 experiments are identified as having lower strength in the distortional mode than the local mode. The increased prevalence of distortional failures in the data on lipped Z's vs. C's is due in part to the ineffectiveness of sloping lip stiffeners and because the researchers systematically varied lip length in these specimens (from no lip up to lip lengths nearly as wide as the flange width) . The specimens with small lips (or no lip at all) are identified as failing in the distortional mode, as the lip length increases local buckling quickly controls – this is accentuated by the fact that the *h/b* ratio is never less than 1.5, and local buckling generally controls for even moderately sized lips in this case.

Table 9 Test to predicted ratio for lipped channels and Z sections (st. dev. in parentheses)

limit states checked*?	L+E	L+E, D	L+E, D			L+E, D+E			L+D, L+E, D+E		
design method**:	A1	A2	B1	B2	B3	C1	C2	C3	D1	D2	D3
Lipped Channels											
Loughlan (1979)	**0.97**	**0.97**	**0.97**	**1.11**	**1.08**	**0.97**	**1.11**	**1.08**	**1.25**	**1.43**	**1.41**
	(0.04)	(0.04)	(0.04)	(0.07)	(0.07)	(0.04)	(0.07)	(0.06)	(0.15)	(0.21)	(0.20)
Miller and Pekoz (1994)	**0.86**	**0.86**	**0.86**	**1.01**	**1.00**	**0.88**	**1.01**	**1.02**	**1.46**	**1.77**	**1.86**
	(0.04)	(0.04)	(0.04)	(0.07)	(0.07)	(0.05)	(0.07)	(0.12)	(0.12)	(0.14)	(0.22)
Mulligan (1983)	**0.86**	**0.86**	**0.83**	**0.94**	**0.92**	**0.84**	**0.94**	**0.92**	**0.94**	**1.06**	**1.08**
	(0.12)	(0.12)	(0.12)	(0.12)	(0.13)	(0.12)	(0.12)	(0.13)	(0.13)	(0.17)	(0.19)
Mulligan (1983) Stub Col.	**1.05**	**1.06**	**1.06**	**1.15**	**1.13**	**1.06**	**1.15**	**1.14**	**1.47**	**1.64**	**1.76**
	(0.06)	(0.06)	(0.06)	(0.09)	(0.11)	(0.07)	(0.09)	(0.11)	(0.21)	(0.37)	(0.50)
Thomasson (1978)	**0.99**	**1.00**	**1.00**	**1.01**	**1.00**	**1.03**	**1.02**	**1.03**	**1.06**	**1.08**	**1.09**
	(0.23)	(0.23)	(0.23)	(0.22)	(0.22)	(0.22)	(0.22)	(0.22)	(0.24)	(0.26)	(0.28)
Z-Sections											
Polyzois at al. (1993)	**0.93**	**0.98**	**0.94**	**0.99**	**0.96**	**0.96**	**1.01**	**0.98**	**1.10**	**1.20**	**1.24**
	(0.10)	(0.14)	(0.14)	(0.13)	(0.13)	(0.16)	(0.15)	(0.15)	(0.23)	(0.26)	(0.29)
All Data	**0.94**	**0.96**	**0.94**	**1.01**	**0.99**	**0.95**	**1.02**	**1.01**	**1.15**	**1.28**	**1.32**
st. dev of all data	(0.13)	(0.14)	(0.15)	(0.14)	(0.15)	(0.16)	(0.15)	(0.16)	(0.27)	(0.34)	(0.39)
weighted st. dev.	(0.09)	(0.10)	(0.11)	(0.11)	(0.12)	(0.12)	(0.12)	(0.13)	(0.20)	(0.25)	(0.29)

* L=Local, D=Distortional, E=Euler

** A1=AISI (1996) Specification, A2=AISI (1996) with a distortional buckling check, B3 and C3 and D3 are direct strength methods, based on finite strip results, with the strength considering different interactions.

Table 10 Test to Predicted Ratios for all 11 Solution Methods, Broken Down by Controlling Limit State

design method:	A1: AISI (1996) Specification								
limit state[1]:	L+E			-			-		
test to predicted stats[2]:	**mean**	std	count	**mean**	std	count	**mean**	std	count
Loughlan (1979)	**0.97**	0.04	13						
Miller and Pekoz (1994)	**0.86**	0.04	13						
Mulligan (1983)	**0.86**	0.12	33						
Mulligan (1983) Stub Col.	**1.05**	0.06	24						
Thomasson (1978)	**0.99**	0.23	19						
Polyzois at al. (1993)	**0.93**	0.10	85						
All Data	**0.94**	0.13	187						

design method:	A2: AISI (1996) Specification with Distortional Check								
limit state[1]:	L+E			D			-		
test to predicted stats[2]:	**mean**	std	count	**mean**	std	count	**mean**	std	count
Loughlan (1979)	**0.97**	0.04	13						
Miller and Pekoz (1994)	**0.86**	0.04	13						
Mulligan (1983)	**0.86**	0.12	33						
Mulligan (1983) Stub Col.	**1.06**	0.06	20	**1.10**	0.09	4			
Thomasson (1978)	**1.00**	0.24	18	**0.98**		1			
Polyzois at al. (1993)	**0.92**	0.10	60	**1.12**	0.12	25			
All Data	**0.93**	0.13	157	**1.11**	0.11	30			

design method:	B1: Effective Width Method with L+E and D Check								
limit state[1]:	L+E			D			-		
test to predicted stats[2]:	**mean**	std	count	**mean**	std	count	**mean**	std	count
Loughlan (1979)	**0.97**	0.04	13						
Miller and Pekoz (1994)	**0.86**	0.04	13						
Mulligan (1983)	**0.83**	0.12	33						
Mulligan (1983) Stub Col.	**1.05**	0.06	19	**1.10**	0.07	5			
Thomasson (1978)	**1.00**	0.24	18	**0.98**		1			
Polyzois at al. (1993)	**0.87**	0.08	47	**1.03**	0.16	38			
All Data	**0.91**	0.14	143	**1.04**	0.15	44			

design method:	B2: Hand Based Direct Strength Method with L+E & D								
limit state[1]:	L+E			D			-		
test to predicted stats[2]:	**mean**	std	count	**mean**	std	count	**mean**	std	count
Loughlan (1979)	**1.11**	0.07	13						
Miller and Pekoz (1994)	**1.01**	0.07	13						
Mulligan (1983)	**0.94**	0.12	33						
Mulligan (1983) Stub Col.	**1.15**	0.09	24						
Thomasson (1978)	**1.01**	0.22	19						
Polyzois at al. (1993)	**0.95**	0.12	60	**1.09**	0.11	25			
All Data	**1.00**	0.15	162	**1.09**	0.11	25			

design method:	B3: Numerical Direct Strength Method with L+E & D								
limit state[1]:	L+E			-			-		
test to predicted stats[2]:	**mean**	std	count	**mean**	std	count	**mean**	std	count
Loughlan (1979)	**1.08**	0.07	13						
Miller and Pekoz (1994)	**0.99**	0.06	12	**1.09**		1			
Mulligan (1983)	**0.92**	0.13	33						
Mulligan (1983) Stub Col.	**1.10**	0.09	20	**1.28**	0.04	4			
Thomasson (1978)	**1.00**	0.23	18	**1.02**		1			
Polyzois at al. (1993)	**0.92**	0.12	60	**1.05**	0.10	25			
All Data	**0.97**	0.14	156	**1.08**	0.12	31			

design method:	C1: Effective Width Method with L+E and D+E Check								
limit state[1]:	L+E			D+E			-		
test to predicted stats[2]:	**mean**	std	count	**mean**	std	count	**mean**	std	count
Loughlan (1979)	**0.97**	0.04	12	**0.94**		1			
Miller and Pekoz (1994)	**0.85**	0.04	8	**0.93**	0.03	5			
Mulligan (1983)	**0.84**	0.12	32	**0.74**		1			
Mulligan (1983) Stub Col.	**1.04**	0.06	18	**1.10**	0.07	6			
Thomasson (1978)	**1.04**	0.25	14	**0.97**	0.10	5			
Polyzois at al. (1993)	**0.87**	0.08	47	**1.07**	0.17	38			
All Data	**0.91**	0.14	131	**1.04**	0.16	56			

design method:	C2: Hand Based Direct Strength with L+E & D+E								
limit state[1]:	L+E			D+E			-		
test to predicted stats[2]:	**mean**	std	count	**mean**	std	count	**mean**	std	count
Loughlan (1979)	**1.12**	0.05	12	**0.94**		1			
Miller and Pekoz (1994)	**1.01**	0.07	13						
Mulligan (1983)	**0.94**	0.12	33						
Mulligan (1983) Stub Col.	**1.15**	0.09	24						
Thomasson (1978)	**1.01**	0.25	14	**1.04**	0.09	5			
Polyzois at al. (1993)	**0.96**	0.12	57	**1.12**	0.15	28			
All Data	**1.00**	0.15	153	**1.10**	0.15	34			

design method:	C3: Numerical Direct Strength Method with L+E & D+E								
limit state[1]:	L+E			D+E			-		
test to predicted stats[2]:	**mean**	std	count	**mean**	std	count	**mean**	std	count
Loughlan (1979)	**1.09**	0.05	12	**1.00**		1			
Miller and Pekoz (1994)	**0.99**	0.06	12	**1.38**		1			
Mulligan (1983)	**0.92**	0.13	33						
Mulligan (1983) Stub Col.	**1.10**	0.10	18	**1.26**	0.06	6			
Thomasson (1978)	**1.07**	0.30	9	**1.00**	0.13	10			
Polyzois at al. (1993)	**0.92**	0.12	60	**1.12**	0.10	25			
All Data	**0.97**	0.15	144	**1.11**	0.14	43			

design method:	D1: Effective Width with L+E, D+E, and L+D Checks								
limit state[1]:	L+E			D+E			L+D		
test to predicted stats[2]:	**mean**	std	count	**mean**	std	count	**mean**	std	count
Loughlan (1979)							**1.25**	0.15	13
Miller and Pekoz (1994)							**1.46**	0.12	13
Mulligan (1983)	**0.94**	0.16	7				**0.94**	0.13	26
Mulligan (1983) Stub Col							**1.47**	0.21	24
Thomasson (1978)	**1.04**	0.25	14				**1.12**	0.24	5
Polyzois at al. (1993)	**0.86**	0.05	11				**1.14**	0.22	74
All Data	**0.96**	0.20	32				**1.19**	0.26	155

design method:	D2: Hand Based Direct Strength with L+E, D+E, & L+D								
limit state[1]:	L+E			D+E			L+D		
test to predicted stats[2]:	**mean**	std	count	**mean**	std	count	**mean**	std	count
Loughlan (1979)							**1.43**	0.21	13
Miller and Pekoz (1994)							**1.77**	0.14	13
Mulligan (1983)	**1.01**	0.16	7				**1.07**	0.17	26
Mulligan (1983) Stub Col							**1.64**	0.37	24
Thomasson (1978)	**1.03**	0.27	12	**1.08**	0.04	2	**1.21**	0.27	5
Polyzois at al. (1993)	**0.88**	0.07	11				**1.25**	0.24	74
All Data	**0.97**	0.20	30				**1.34**	0.33	155

design method:	D3: Numerical Direct Strength with L+E, D+E, and L+D								
limit state[1]:	L+E			D+E			L+D		
test to predicted stats[2]:	**mean**	std	count	**mean**	std	count	**mean**	std	count
Loughlan (1979)							**1.41**	0.20	13
Miller and Pekoz (1994)							**1.86**	0.22	13
Mulligan (1983)	**0.99**	0.21	4				**1.09**	0.19	29
Mulligan (1983) Stub Col							**1.76**	0.50	24
Thomasson (1978)	**1.07**	0.30	9	**0.95**	0.14	5	**1.27**	0.28	5
Polyzois at al. (1993)							**1.24**	0.29	85
All Data	**1.05**	0.27	13				**1.35**	0.39	169

[1] L=Local buckling, D=Distortional buckling, E=Euler (overall) buckling, L+E =Limit State that consider Local buckling interaction with Euler (overall) buckling, etc.

[2] test to predicted ratios are broken down by the controlling limit state

8.2 AISI Performance (A1)

Experimental data on lipped channels and Z sections indicates that the overall performance of the current AISI (1996) Specification is good, but 6% unconservative.

Within the limitations of the experimental data, the AISI Specification does not exhibit poor performance related specifically to the distortional mode. The addition of a separate distortional check (method A2) provides little change to the results; compare A1 and A2 in Table 9, or note in Table 10 that the distortional check almost never controls (only 5 times in 102 lipped channels). Further, Figure 20 presents the test to predicted ratio for the AISI method vs. the ratio of the distortional slenderness/local slenderness for the data. As the ratio of the distortional slenderness/local slenderness increases the distortional mode becomes more prevalent. No trend exists in the data to suggest that members more prone to distortional modes are problematic for the AISI Specification. (Note, slenderness is the square root of the inelastic Euler buckling stress F_n divided by the critical buckling stress for the appropriate mode.)

Systematic error does exist in the current AISI Specification approach for columns. Investigation of the performance vs. *h/t*, or *h/t·h/b* shows this behavior. Consider Figure 21 which shows the data for lipped channels vs. the slenderness of the web, *h/t*. As *h/t* increases the AISI method is prone to yield unconservative solutions. If *h/t* and *h/b* is high, such that the web is contributing a large percentage to the overall strength, then the behavior is more pronounced. This behavior is primarily one of local web/flange interaction, not distortional buckling. Since the AISI method uses an element approach, *no matter how high the slenderness of the web becomes* it has no effect on the solution for the flange.

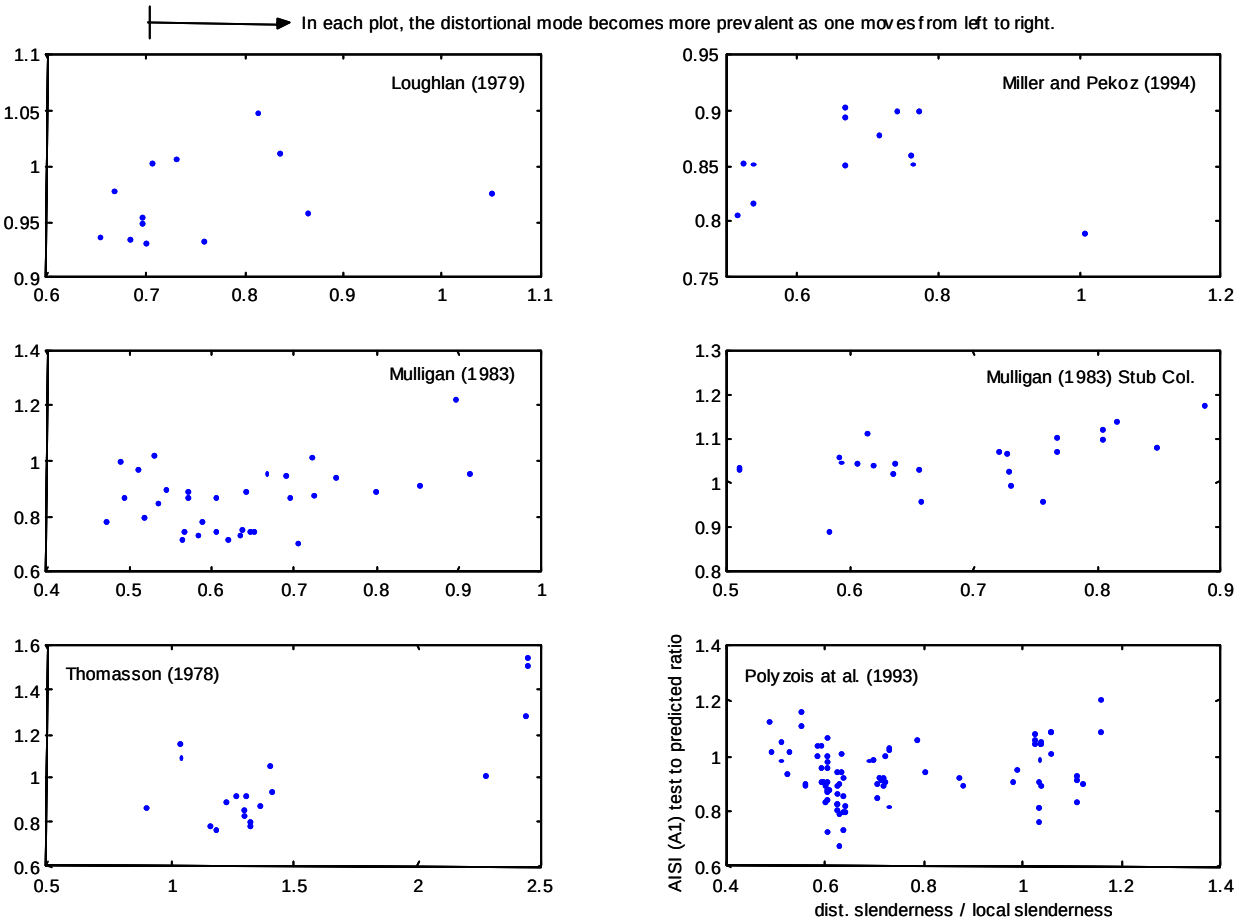

Figure 20 Performance of the AISI Specification (A1) vs. distortional/local slenderness

The data on Z-sections performed by Polyzois et al. (1993) shows another aspect of the AISI Specification that is inconsistent and in some cases unconservative. For small to intermediate lip lengths the AISI prediction in some tests is significantly unconservative (e.g., $d \sim 20$ in Figure 22). For longer lip lengths the Specification under-predicts the observed strength. The reduction in the AISI strength prediction occurs due to an expression that decreases k as $d/b > 0.25$ (expression B4.2-8 in AISI (1996) Specification). In addition the double reduction on the lip, first for its own effective width, then due to the ratio of supplied to adequate stiffener moment of inertia further penalizes longer lips. For longer lips the Specification appears overly conservative.

Performance of the AISI Specification is generally good, and no distinct problems with respect to distortional buckling are identified by the studied data. However, members with large h/t, particularly when $h/b \sim> 2$ tend to have unconservative predictions. Experimental data on Z-sections indicates that intermediate length lip stiffeners may have unconservative predictions while; at the same time predictions for long lip lengths are generally overly conservative.

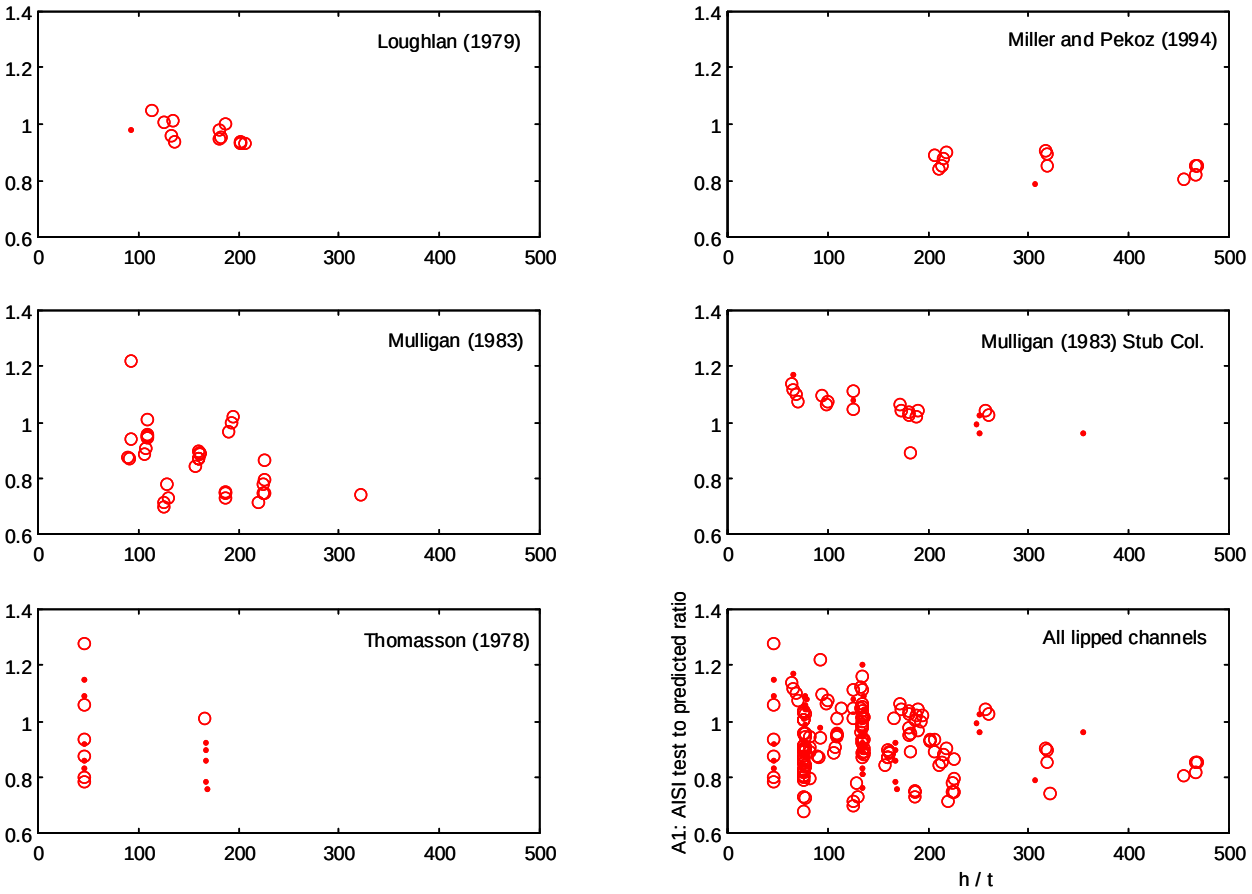

Figure 21 Performance of the AISI Specification (A1) vs. web slenderness (circles indicate members preficted to fail in a local mode by method C3, dots indicate members predicted to fail in a distortional mode by method C3)

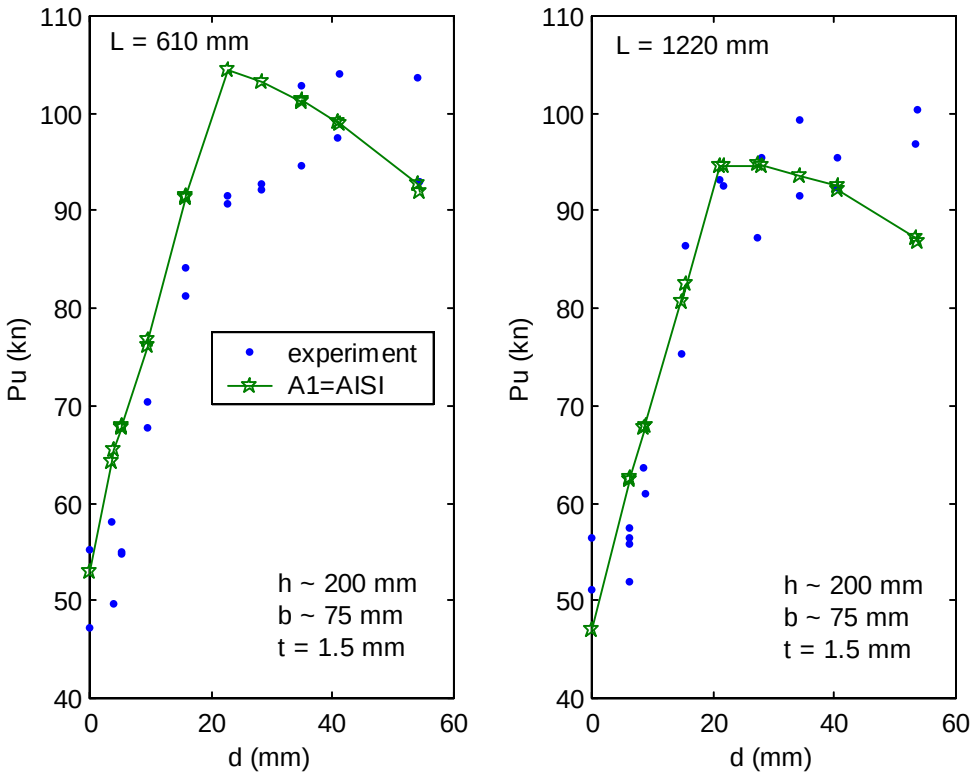

Figure 22 Performance of the AISI Specification for Z Sections

8.3 AISI with a distortional check (A2)

The experimental data on lipped C and Z Sections indicates that the AISI Specification would not significantly benefit from the addition of a separate distortional buckling check. Error in the current AISI Specification is not a function of distortional buckling, and instead relates primarily to web/flange interaction in local buckling Existing rules work reasonably well for the majority of simple lipped C and Z Sections.

However, rack sections, sections with intermediate web stiffeners, and a variety of other optimized shapes which are more prone to distortional buckling (see Figure 18) still require accurate design methods. These shapes would benefit from the proper inclusion of distortional buckling into the Specification, even a simple additional check, such as investigated in this design approach.

8.4 Alternative Effective Width Method B1

The current AISI Specification uses an effective width method for determining strength in local buckling. However, the effective width is based on expressions, such as those in AISI Specification Section B4.2 for edge stiffened elements, that include aspects of local buckling and distortional buckling. If distortional buckling is treated separately, then only local buckling need be considered in determination of the local buckling effective width. For example, in a lipped channel, the flange would always use k = 4, for local buckling, instead of a modified *k* value.

This basic approach is investigated in methods B1, C1 and D1 - considering various interactions amongst the modes. The simplest of which, B1, uses a separate check for distortional buckling and considers local and Euler buckling interaction. Figure 23 shows how B1 predicts the experiments on Z sections. The predicted strength is the minimum of the distortional buckling curve and the local buckling curve (which includes Euler buckling interaction.) The method provides a reasonable upper bound to the data and demonstrates that if a separate distortional check is made, the complicated rules for determining *k*, in Specification section B4.2 could be abandoned and a simple *k* = 4 value could be used for local buckling of edge stiffened elements.

The results of Table 9 show that in general this approach (B1) can work as well as existing design rules. Table 10 shows that members identified to fail in the distortional mode are well predicted by the method; however, members failing in the local mode are not predicted as accurately. The systematically unconservative predictions for lipped C's with high web slenderness (*h/t*) exhibited by the AISI Specification is slightly reduced using method B1, but not eliminated. The local web/flange interaction that occurs in the members with high *h/t* ratios is not well predicted by this method, because the element based effective width methods assume the *k* (plate buckling coefficient) for each element is independent.

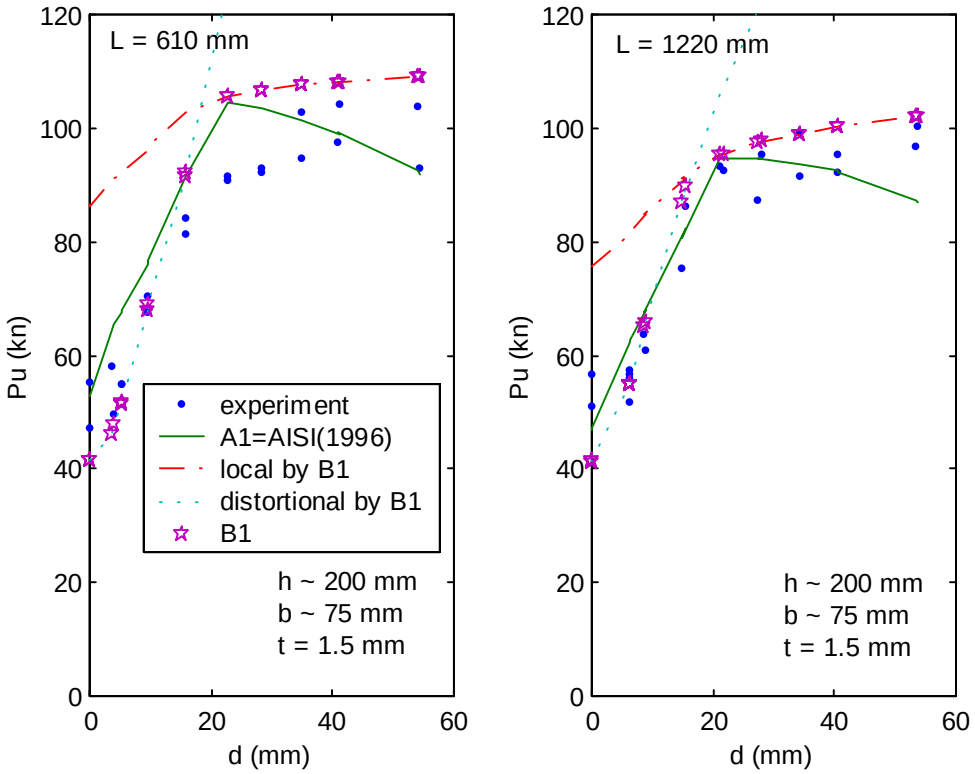

Figure 23 Performance of method B1 for sample of Z-Section Data

8.5 Hand Solutions, Direct Strength Method B2

Hand solutions for the elastic local and distortional buckling of C's and Z's that account for the interaction of the elements are available (see Appendix B for examples). Those hand solutions may be used to determine the slenderness in the local and distortional modes. Two different strength curves are postulated, one for local buckling (e.g., if no Euler interaction $P_n/P_y=(1-0.15(P_{crL}/P_y)^{0.4})(P_{crL}/P_y)^{0.4}$) and one for distortional buckling (e.g., if no Euler interaction $P_n/P_y=(1-0.25(P_{crD}/P_y)^{0.6})(P_{crD}/P_y)^{0.6}$) in order to predict the strength in these modes.

For the lipped C and Z section data the performance of the strength curves may be gauged in a simple plot of slenderness vs. strength, as shown in Figure 24 for method B2 (statistical rather than graphical summaries are in Table 9 and Table 10). Overall the method works well, and given typical scatter in column data, appears to be a good predictor over a wide range of slenderness. Examination of Table 10 shows that the increased accuracy of the method (over methods A1, A2 and B1) occurs due to improvements in the local buckling prediction – i.e. web/flange and flange/lip interaction are included in the local buckling calculation of method B2.

Figure 25 shows how the results od method B2, for the same Z section data in which the lip length is systematically increased. The presented method (B2) provides a good average prediction of the experimental data. Examination of all the experiments with respect to *h/t* and *h/t·h/b* as well as other variables reveals no systematic error in the method. Test to predicted ratios (Table 9) indicate that the basic approach (methods B2, C2, and D2) is sound, as long as local and distortional interaction (method D2) is ignored.

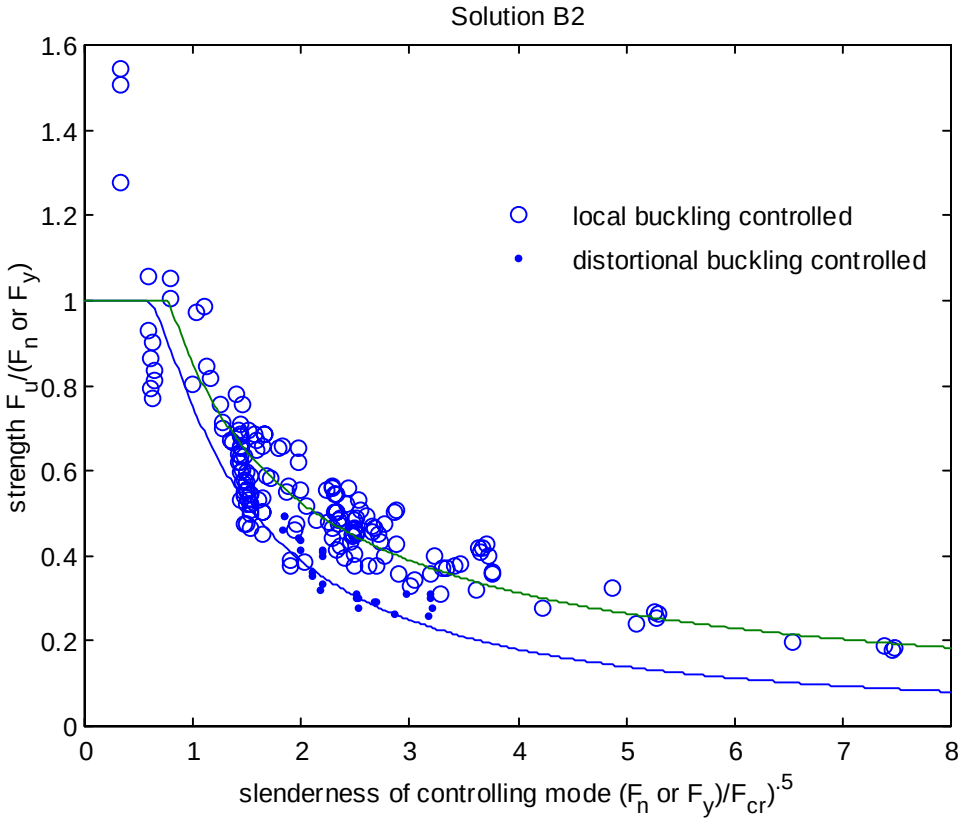

Figure 24 Slenderness vs. strength for method B2

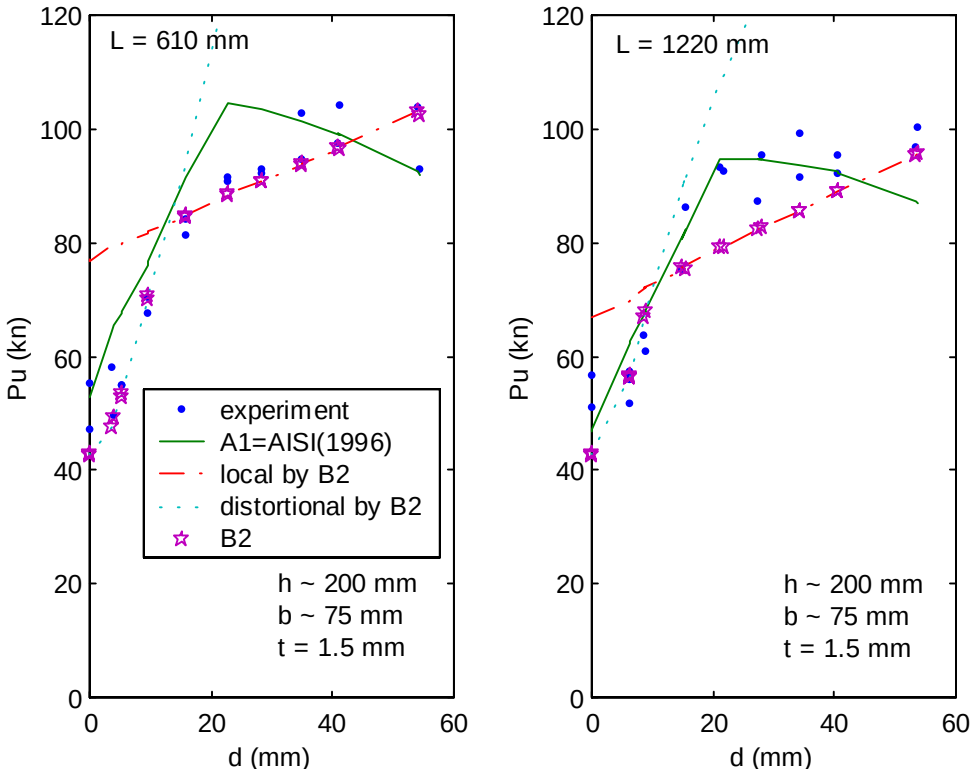

Figure 25 Performance of method B2 for sample of Z-Section data

8.6 Numerical Solutions, Direct Strength Method B3

The Direct Strength Method postulates that if the elastic critical buckling loads in the local and distortional mode are known for the entire member, this may be used to directly determine the member strength. A hand method implementation of this approach (method B2) agrees well with the experiments. Numerical implementation, in which the local and distortional buckling loads are determined from finite strip analysis performs as well or better. Consider a plot of slenderness vs. strength for the collected data for prediction method B3 (Figure 26).

Comparison against the Z section data is given in Figure 27. Figure 27 and Figure 22 underscore that the large difference between the various presented design methods is a function of how local buckling interaction is handled, not how distortional buckling is dealt with. Table 10 also demonstrates this same point, as the test to predicted ratios for local bucking are far more influential in assessing the overall accuracy of the method. Method B3 provides a good average prediction of the experimental data. Examination of all the experiments with respect to *h/t* and *h/t·h/b* as well as other variables reveals no systematic error. Test to predicted ratios (Table 9) indicate that overall the basic approach (methods B3, C3, and D3) is sound, as long as local and distortional interaction (method D3) is ignored.

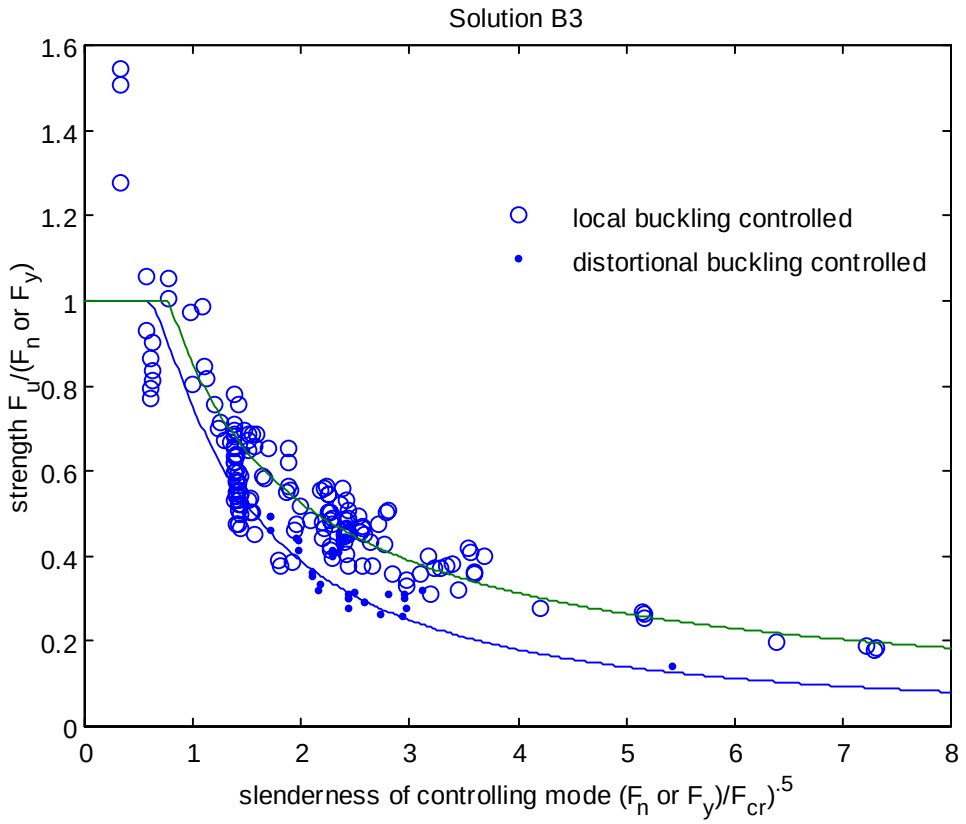

Figure 26 Slenderness vs. strength for C and Z sections, method B3

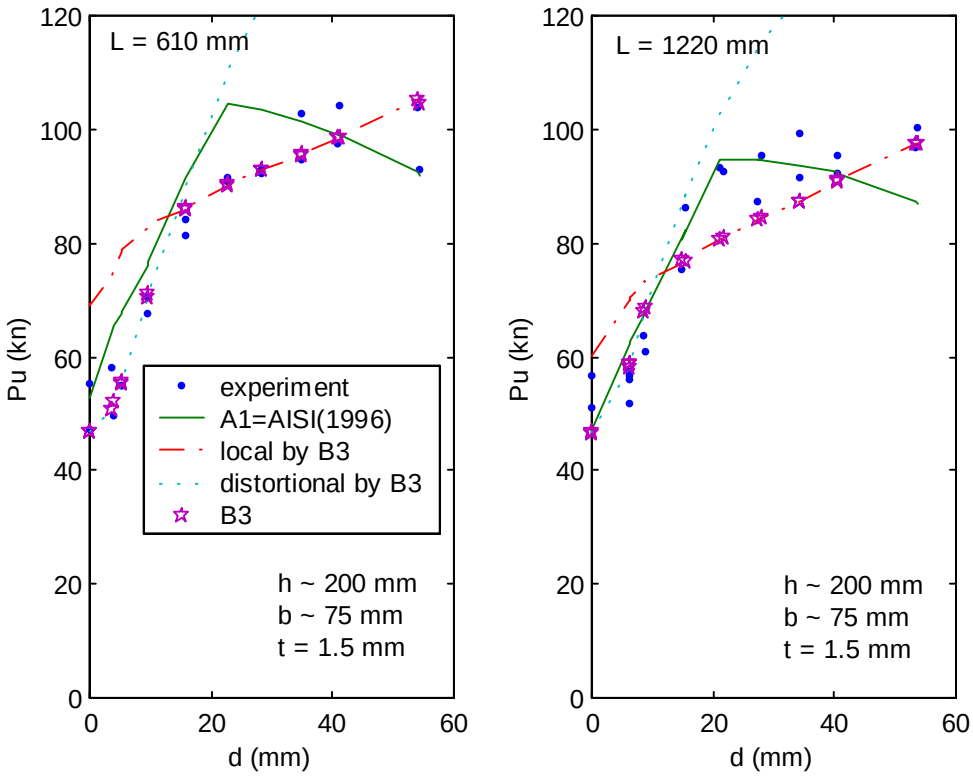

Figure 27 Performance of method B3 for sample of Z-Section data

8.7 Methods which allow Distortional and Euler Interaction (C1, C2, C3)

Design methods C1, C2, and C3 are nearly identical to their counterparts, methods B1, B2, and B3 respectively, except that in the strength calculation for distortional buckling the possibility of interaction with Euler (overall long-column) buckling is recognized (see Appendix D for design examples). Comparing the mean test to predicted ratios in Table 9 shows that for the studied experimental data of lipped C and Z sections little overall difference occurs when distortional and Euler interaction is considered. Looking at the more detailed results in Table 10 shows that the local buckling predictions remain essentially unchanged and the distortional buckling predictions are slightly more conservative (as expected). Interaction of distortional buckling with Euler buckling cannot be definitively recognized nor rejected from the available data.

For members with small edge stiffeners distortional and Euler interaction seems plausible, because the deformations and wavelengths involved are similar to the ones that initiate local and Euler buckling interaction (in pin-ended columns). However, for members with intermediate stiffeners or other additional folds, the amount of interaction for distortional and Euler buckling would seem to be much lower, particularly given the long wavelengths that distortional buckling occurs at in these members. For example, the experimental data on channels with intermediate stiffeners and racks with large compound lips (Figure 18) ignores this interaction.

Including Euler interaction in the distortional buckling calculation is conservative. Further, the inclusion of Euler buckling does not complicate the procedure, since it must already be considered for the local mode. A plot of slenderness vs. strength for method C3 is given in Figure 28, comparison with Figure 26 provides a means to assess the impact of including the interaction. In Figure 28 the slenderness is defined as the square root of the inelastic Euler column buckling stress (F_n) divided by the local or distortion buckling stress, and strength is simply normalized by F_n. (Note, Figure 28 is identical for load (P) or stress (f) since ratios are used for both the x and y axes).

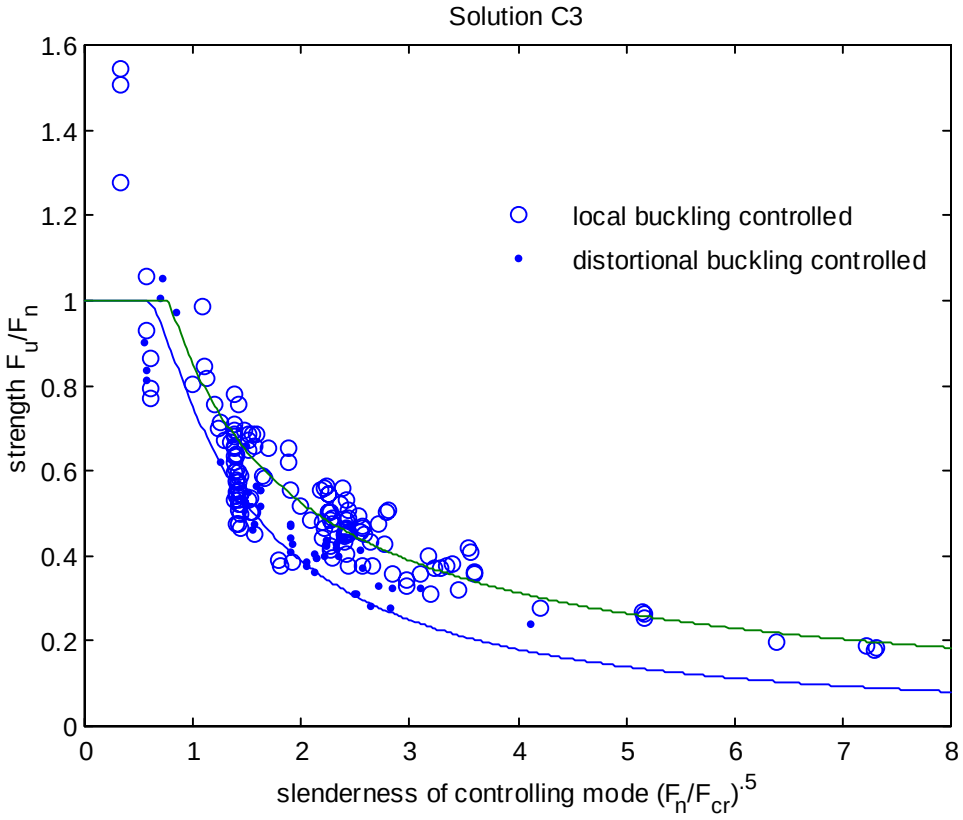

Figure 28 Slenderness vs. strength for C and Z sections, method C3

8.8 Methods which allow Local and Distortional Interaction (D1, D2, and D3)

The "D" methods (D1, D2 and D3) allow local and distortional interaction by setting the limiting inelastic stress for local buckling to the inelastic distortional buckling stress (see Appendix D for design examples). The "D" methods perform poorly (overly conservative) – see Table 9 and Table 10. In the majority of cases local plus distortional interaction is identified as the controlling limit state, but predicted strengths are significantly lower than tested capacities. This evaluation does not indicate that no interaction exists between these two modes, but in the available data, local and distortional interaction does not appear significant.

Based on this finding it is recommended that local and distortional interaction be ignored for routine design. Note, other data may indicated interaction between these two modes, for example as stated earlier, some evidence exists for perforated rack columns that local and distortional modes may interact (Baldassino and Hancock 1999).

9 Performance for Additional Experimental Data

9.1 Lipped Channel with Web Stiffeners

Thomasson (1978) tested a series of cold-formed columns with up to two stiffeners in the web, with geometry as shown in Figure 29 and summarized in Table 11. (The members without intermediate web stiffeners are included in the group of experimental data on lipped channels previously presented.) Thomasson investigated channels with very slender webs, flanges, and lips. The thickness was as low as 0.63 mm (0.025 in.) in some specimens, which lead to the high width to thickness ratios, presented in Table 11.

Figure 29 shows attachments to the lips of the channels with one or two intermediate stiffeners. When Thomasson initially tested the specimens with an intermediate stiffener they buckled in a distortional mode:

> "The provision of one or two stiffeners in the wide flange [the web] confers on the panel both an elevated load bearing capacity and an elevated stiffness. The consequences of improving the stiffness of the wide flange were not entirely favourable. . ..In order that the improved properties of the wide flange may be utilised, steps must be taken to prevent the occurrence of the torsional mode. By connecting the narrow flanges of the panels by means of 30 x 3 mm flats at 300 mm centres, the symmetrical torsion mode [Figure 30 (a)] was eliminated. This measure does not prevent the occurrence of the anti-symmetrical mode [Figure 30 (b)]." Thomasson (1978)

Numerical prediction of the elastic buckling stress (load) of the anti-symmetrical distortional mode may be approximated by modeling only ½ of the member and enforcing anti-symmetry at mid-width of the web.

Due to the more complicated cross-section only design methods B3 and C3, the numerical Direct Strength methods, are investigated for this data. The test to predicted ratios presented in Table 12 indicate that (a) the experimental results are generally lower than the predicted values and (b) including distortional interaction with Euler buckling (method C3) provides better mean predictions of the strength. The slenderness vs. strength for this data presented in Figure 31 indicates that including the long column interaction (method C3) also provides a different prediction of the failure mode for a number of the members.

The tested members are quite slender. Nonetheless, the predicted strength without intermediate web stiffeners is excellent for methods B3 or C3, see Table 9. In the members with intermediate web stiffeners, the addition of the straps to restrict symmetrical distortional buckling makes prediction of the strength slightly more complicated. Nonetheless, predictions are adequate, particularly if long column interaction (method C3) is included.

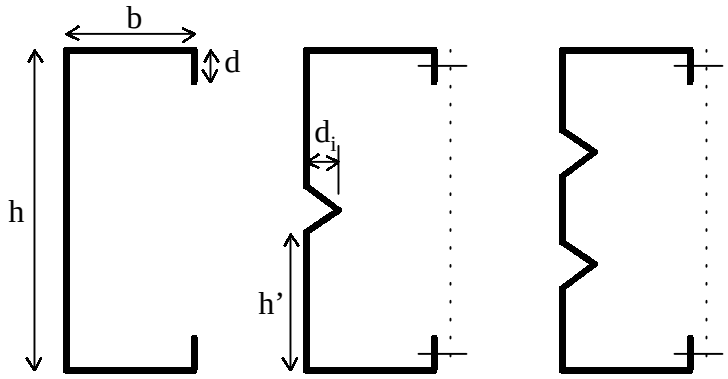

Figure 29 Geometry of lipped channels tested by Thomasson (1978)

Table 11 Summary of geometry of lipped channels tested by Thomasson (1978)

	h/b		h/t		b/t		d/t		
	max	min	max	min	max	min	max	min	count
Thomasson (1978)	3.1	3.0	489	205	160	68	33	14	46
					d_i/d		h'/t		
					max	min	max	min	count
	no intermediate web stiffeners				-	-	-	-	14
	one intermediate web stiffener				0.94	0.39	222	91	16
	two intermediate web stiffeners				0.94	0.47	145	57	16

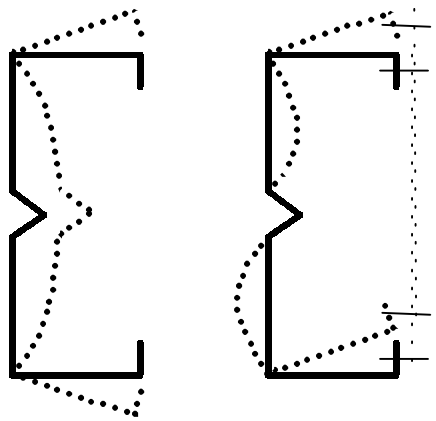

Figure 30 Distortional buckling modes (a) modeobserved in initial testing with web stiffener in place (b) mode observed after addition of flat bars connecting lip stiffeners

Table 12 Test to predicted ratio for Thomasson (1978) channels with intermediate web stiffeners

limit states checked?	L+E	L+E, D	L+E, D			L+E, D+E			L+D, L+E, D+E		
design method:	A1	A2	B1	B2	B3	C1	C2	C3	D1	D2	D3
Channels with int. stiffeners and straps* Thomasson (1978)											
1 int. web stiffener	-	-	-	-	**0.83**	-	-	**0.85**	-	-	-
	-	-	-	-	(0.10)	-	-	(0.07)	-	-	-
2 int. web stiffeners	-	-	-	-	**0.85**	-	-	**0.95**	-	-	-
	-	-	-	-	(0.12)	-	-	(0.16)	-	-	-

* lips of edge stiffeners strapped together, thus restricting symmetrical distortional buckling

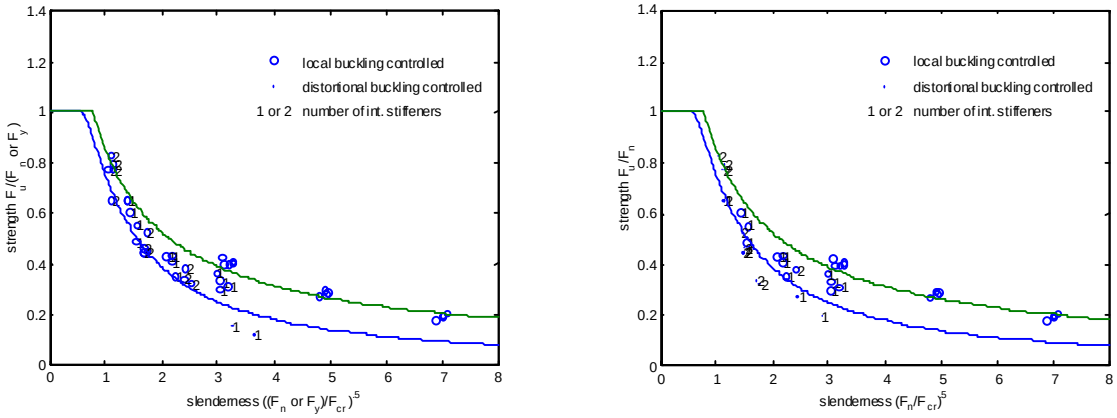

(a)method B3 (b) method C3

Figure 31 Slenderness vs. strength for Thomasson(1978) tests

9.2 All available data

The Thomasson (1978) data and The University of Sydney experimental data (see Section 5.2) is added to the data on lipped C and Z sections. The slenderness vs. strength plot for method C3 is completed in order to provide a presentation of the overall strength prediction for the Direct Strength Method for available column data. Though scatter certainly exists the plot demonstrates that such an approach is viable as a general method for prediction of the

strength of cold-formed steel columns in local, or distortional buckling with consideration of interaction with long column Euler buckling.

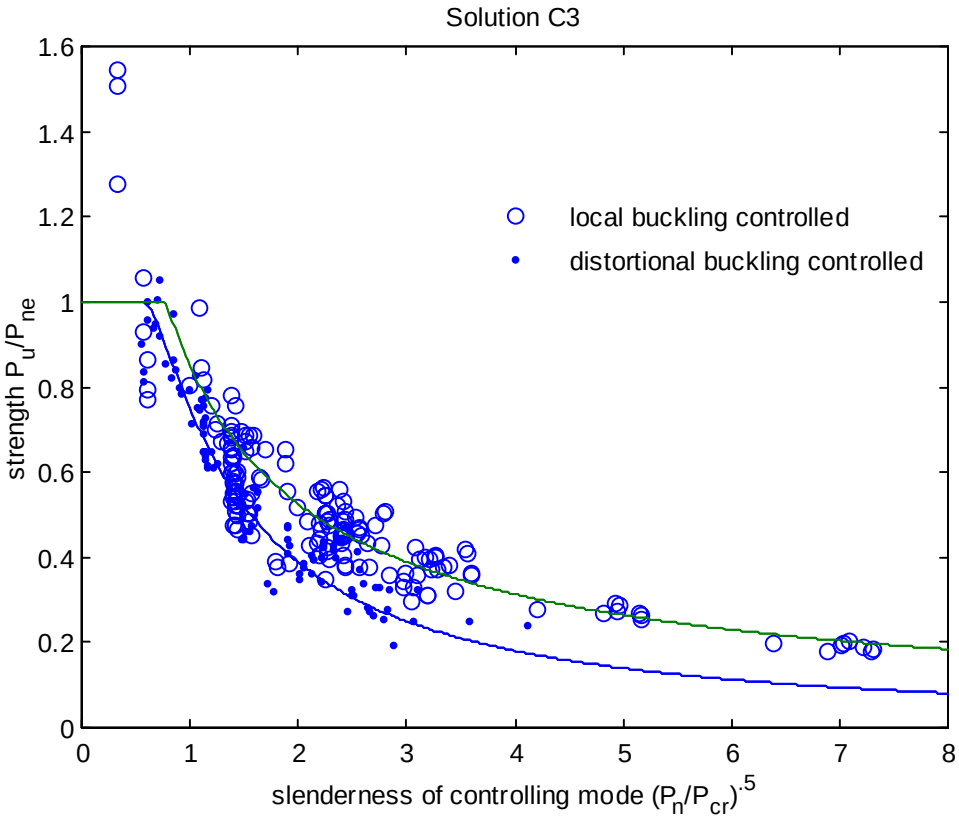

Figure 32 Slenderness vs. strength all available column data (C's, Z's, C's with int. web stiffeners, racks, racks with compound lips)

10 Discussion

10.1 Reliability of examined methods (ϕ factors)

The reliability of the 11 design methods was assessed by calculating the resistance factor (ϕ) for a β of 2.5 via the guidelines of Section F in the AISI Specification. The results are given in Table 13. Variability in the data is relatively high, and the resulting ϕ factors are consistent with current practice of $\phi = 0.85$.

If local and distortional buckling are treated as different limit states then the possibility of using two different ϕ factors exists. The experimental data suggests lower ϕ factors for local buckling limit states than distortional buckling. However, this does not reflect the variability in the data (Table 10 shows the variability in the 2 methods is generally about the same – if not a little higher for distortional failure modes) but rather reflects the higher test to predicted ratios for currently proposed formula in the distortional mode.

Numerical studies presented in Section 5.1 suggest that distortional failures have a greater imperfection sensitivity and thus lower ϕ factors may be needed for this mode. This observation may be true, but it is not borne out by this data. Continued use of $\phi \sim 0.85$ appears appropriate for cold-formed steel columns.

Table 13 Calculated Resistance Factors (ϕ) for the 11 Methods by Limit State

Design method	L+E	D or D+E	L+D	All Data[1]
A1: AISI (1996) Specification	0.79			**0.82**
A2: AISI (1996) plus distortional check	0.78	0.94		**0.83**
B1: Effective width with distortional check	0.75	0.84		**0.81**
B2: Direct Strength by hand w/ dist. check	0.82	0.92		**0.86**
B3*: Direct Strength numerical wi/ dist. check	0.79	0.90		**0.84**
C1: same as B1 but consider D+E interaction	0.75	0.84		**0.81**
C2: same as B2 but consider D+E interaction	0.82	0.89		**0.86**
C3*: same as B3 but consider D+E interaction	0.80	0.89		**0.84**
D1: same as C1 but consideer D+L interaction	0.72		0.81	**0.88**
D2: same as C2 but consider D+L interaction	0.73	0.99	0.80	**0.89**
D3: same as C3 but consider D+L interaction	0.66	0.70	0.70	**0.85**

[1] resistance factor calculations for "all data" use a weighted standard deviation, i.e., the standard deviation for all the data is weighted by the number of samples conducted by each researcher.
* resistance factors calculated for methods B3 and C3 include Thomasson's data as well as all the cited University of Sydney data. Other methods only include the lippped channel and Z's used in this report.

10.2 Understanding when the distortional mode is prevalent – redux

Section 4 of this report provides elastic buckling analysis to answer the question: when is the distortional mode prevalent? Experiments suggest ultimate strength in the local and distortional mode is different, therefore elastic buckling analysis does not provide a complete answer to the above question. The overall pervasiveness of distortional buckling may be assessed by examination of Table 10, which shows the predicted number of failures in the competing modes. For the majority of the studied members local buckling is the predicted failure mode.

A parametric study of member dimensions ranging from *h/b* of 0.1 to 6, *d/b* from 0.01 to 0.5 and *b/t* of 30, 60 and 90 with f_y = 50 ksi is performed using the Direct Strength design method B2 to further investigate ultimate strength in the two modes. The mode with the lower strength is identified in Figure 33. For each *b/t* ratio (30, 60 and 90) figures are provided as a function of *h/b* vs. *d/b* as well as *h/t* vs. *d/t*. Note these figures are dependent on the yield stress selected as well as the dimensional ratios. The difficulty of ascribing simple dimensional limits to determine when local or distortional buckling will control is conveyed by the complexity and changing nature of the border that separates the two limit states in Figure 33.

The distortional mode controls the predicted strength over a relatively large range of dimensions. Members with stocky flanges (fully effective) are more prone to distortional failures than those with slender flanges; however as we learned in Figure 2 there is a limit to this line of thinking, flanges should not be too wide nor too narrow. In most cases members with short lips are prone to distortional failures; however the boundary of what a “short” lip depends on the other dimensions of the column and the yield stress. The border between local and distortional for members with high *h/b* ratios is somewhat misleading, because local and distortional buckling of very narrow members are quite similar phenomena – almost completely driven by the web deformation.

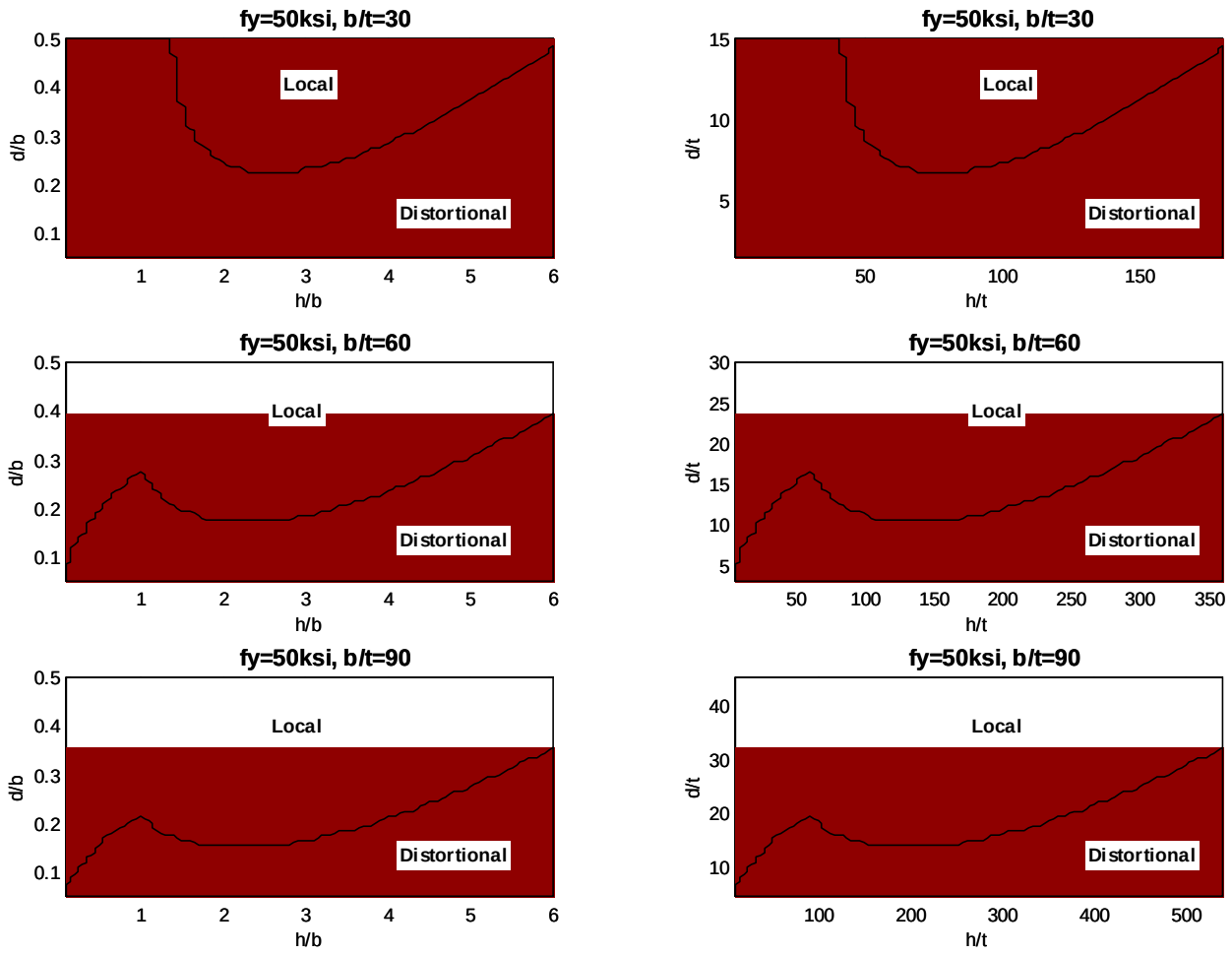

Figure 33 Predicted Failure Modes based on Direct Strength Design Method B2

10.3 Restriction of the Distortional Mode

One factor not explicitly discussed in the majority of this work is the restriction of the distortional mode through bracing or other means. Attachments to sheeting, as well as discrete braces may be used to hinder the distortional mode and thus increase the strength of the member. The analysis of Thomasson's tests in Section 9.1 provides insight on how to use anti-symmetry in numerical analysis for certain special cases of restricted distortional buckling; however, general guidance on including bracing or other attachments that restrict the distortional mode is lacking.

Completely ignoring bracing that restricts the distortional mode can lead to overly conservative design. For discrete braces the best current practice is to compare the unbraced length with the half-wavelength of the mode. If the unbraced length is less than the half-wavelength then it may be used in the hand formulas for prediction of the distortional buckling stress – or the shorter unbraced length may be directly considered in the numerical analysis. The bracing should restrict the rotation of the flange and cause the buckling wave to occur in the unbraced segment.

10.4 Specification Directions?

The current AISI Specification has at least 4 paths that can be taken to address the findings of this work:

1. do nothing / add commentary language only,
2. add an additional strength check for distortional buckling on top of the existing Specification methods,

3. remove section B4.2 and instead always use k=4 for local buckling of edge stiffened elements, and then add a distortional check,
4. adopt a completely new procedure (hand or numerical) which accounts for interaction amongst the elements for local buckling and includes a check on distortional buckling.

Option 1

As the data shows (Table 9) doing nothing, i.e., no change to the Specification, will work reasonably well for a variety of conventional situations. Commentary, or even dimensional limits, could be added to indicate that members with high web slenderness and narrow flanges are likely to yield unconservative solutions with current methods due to local buckling interaction, and members with low web slenderness and wide flanges (shapes approaching square) are likely to yield unconservative solutions with current methods due to distortional buckling. The expressions in B4.2 could even be tweaked to eliminate some of the problems demonstrated in Figure 22 for intermediate length lip stiffeners. However, inherent in this approach is the fact that local buckling interaction (web/flange, flange/lip) and distortional buckling are currently ignored. Further, innovations such as adding stiffeners in the web, or using more efficient stiffening lips are retarded by continued use of current approaches.

Option 2

If distortional buckling was the primary problem with strength predictions for columns then adopting a distortional check on top of current Specification rules would be a viable fix, but it is not. The addition of a distortional check without further modification to the Specification will only complicate, not improve, design. This option should be rejected.

Option 3

Current use of the effective width approach in the Specification essentially necessitates an element by element treatment of the member. If this method is to be maintained the best approach is to simplify the local buckling portion of the procedure (remove section B4.2 and replace with k = 4) and add a distortional buckling check (this is method B1 or C1). Similar design procedures have been proposed for distortional buckling of beams (Hancock et al. 1996, Schafer and Peköz 1999) and shown to provide reliable predictions. This solution accounts for issues related to distortional buckling effectively, but ignores problems related to local buckling interaction.

Option 4

Adopting completely new procedures for cold-formed steel column design requires significant changes in current practice and thinking. The member based, or Direct Strength, methods (B2, C2, D2 and B3, C3, D3) that are investigated herein do not fit well in the current Specification methodology. Instead of breaking the design of a member into detailed calculations of each element the entire cross-section is treated as a whole. “Treating the member as a whole” implies that calculations for local and distortional buckling properly consider the interaction of the elements making up the cross-section. Closed-form expressions and numerical methods are provided for completing this task. The elastic buckling information is used in combination with strength curves to generate the capacity for the member. The accuracy of methods B2, B3, C2, and C3 demonstrate the viability of this approach.

Adoption of the Direct Strength method holds several advantages over current methods: calculations do not have to be performed for individual elements, interaction of the elements in both local and distortional buckling is accounted for, distortional buckling is explicitly treated as a unique limit state, an obvious means for introducing rational analysis through numerical prediction of elastic buckling is provided, and a rational analysis procedure is provided for members with stiffener configurations or other geometries that current rules do not apply to. The Direct Strength method removes systematic errors that exist in the current AISI (1996) method. The method provides a means for integrating known behavior into a straightforward design procedure and should increase innovation of cold-formed steel member cross-sections.

10.5 Recommendations

Based on the findings of this report the following three recommendations are made for improving current practice in cold-formed steel design.

1. Proposed for immediate adoption:

The commentary in AISI Specification Section B4.2 should be revised to provide general guidance on member cross-sections that may be unconservatively predicted by current design methods. Updated references to research that provide design methods for local and distortional buckling should be added. (see Appendix F.1).

2. Proposed for interim adoption

As long as the AISI Specification still follows effective width procedures it is proposed that the existing rules for B4.2 be removed, to be replaced with k = 4 for local buckling of edge stiffened elements and a separate distortional buckling check for all members which have edge stiffened elements in the cross-section be added. (Thus, this recommendation is for interim adoption of design method C1, see Appendix D for a full example and Appendix F.2 for proposed Specification language – this procedure has previously been shown to work for beams as well as columns, see discussion in the previous section).

3. Proposed for long-term adoption and interim adoption as an alternative procedure

Adopt the Direct Strength method for the design of columns as an alternative design procedure, and move towards this procedure in the future. Design method C2 provides a closed-form, "hand" implementation of this method and design method C3 provides the same method with numerical analysis via the finite strip method for predicting the elastic buckling. Method C3 is proposed for adoption with a rational analysis clause to be used for prediction of the elastic buckling loads. The design formula of method C2 could be provided in an Appendix as one form of rational analysis, finite strip and finite element analysis would be other acceptable forms of rational analysis for prediction of elastic buckling. (see Appendix D for complete design examples using methods C2 and C3 and Appendix F.3 for proposed Specification language).

10.6 Industry Impact of Adopting Recommendations

The following discussion relates primarily to changes in the strength prediction of cold-formed steel members due to adoption of the proposed methods. Detailed discussions of the errors in current methods and the advantages of the proposed methods can be found in Section 8 and 9.

Impact of Proposal 1 "for immediate adoption"

Adding additional commentary language will not change the letter of the Specification, but it may change the interpretation slightly. Recognizing the limitations of the current methods in the commentary at least gives the user some knowledge of current findings and the additional references provide guidance as to where more information can be obtained.

Impact of Proposal 2 "for interim adoption"

Adoption of Proposal 2 (in essence, design method C1) will make local buckling calculations simpler - but it will add significant effort to the design due to calculation of the distortional buckling stress. Due to its complexity, the addition of a separate distortional buckling check will encourage a rational analysis clause. This method generally encourages better designs by explicitly recognizing and calculating the distortional mode.

The impact on strength predictions is provided in the detailed summary in Appendix E – which includes a column which compares methods C1 (Proposal 2) to A1 (current AISI 1996 method), and in Figure 34 which plots the ratio of the two methods vs. different geometric quantities. Compared to the current AISI (1996) method adoption of method C1 will favor members with longer lips, and discourage members with small lips. Members with lip length to flange width ratios (*d/b*) less than 0.2 may anticipate significant reductions in strength, while members with *d/b* greater than 0.4 may see large increases. The overall average impact on test to predicted ratios for the studied members is less than 1%.

Impact of Proposal 3 "for long-term adoption and interim adoption as an alternative procedure"

Adoption of the Direct Strength method holds several advantages over current methods: calculations do not have to be performed for individual elements, interaction of the elements in both local and distortional buckling is accounted for and thus systematic error in current methods is removed, distortional buckling is explicitly treated as a unique

limit state, an obvious means for introducing rational analysis through numerical prediction of elastic buckling is provided, and a rational analysis procedure is provided for members with stiffener configurations or other geometries that current rules do not apply to. The method provides a means for integrating known behavior into a straightforward design procedure and should increase innovation of cold-formed steel member cross-sections.

The impact on strength predictions is provided in the detailed summary in Appendix E – which includes a column which compares methods C3 (Proposal 3) to A1 (current AISI 1996 method), and in Figure 35 which plots the ratio of the two methods vs. different geometric quantities. The Direct Strength Method (method C3) provides markedly different strength predictions than current methods. In the studied members of lipped C's and Z's the predicted strength can be as much as 16% higher than the current AISI (1996) method, but on average adoption entails a strength loss of 7%. Compared to the current AISI (1996) method, narrow members (high *h/b*) with slender webs (high *h/t*) and short lips (low *d/b*) will be specifically discouraged. Members with longer lips (higher *d/b*) are encouraged. The method removes systematic error that exist in the current AISI (1996) approach and the overall test to predicted ratio is 1.01.

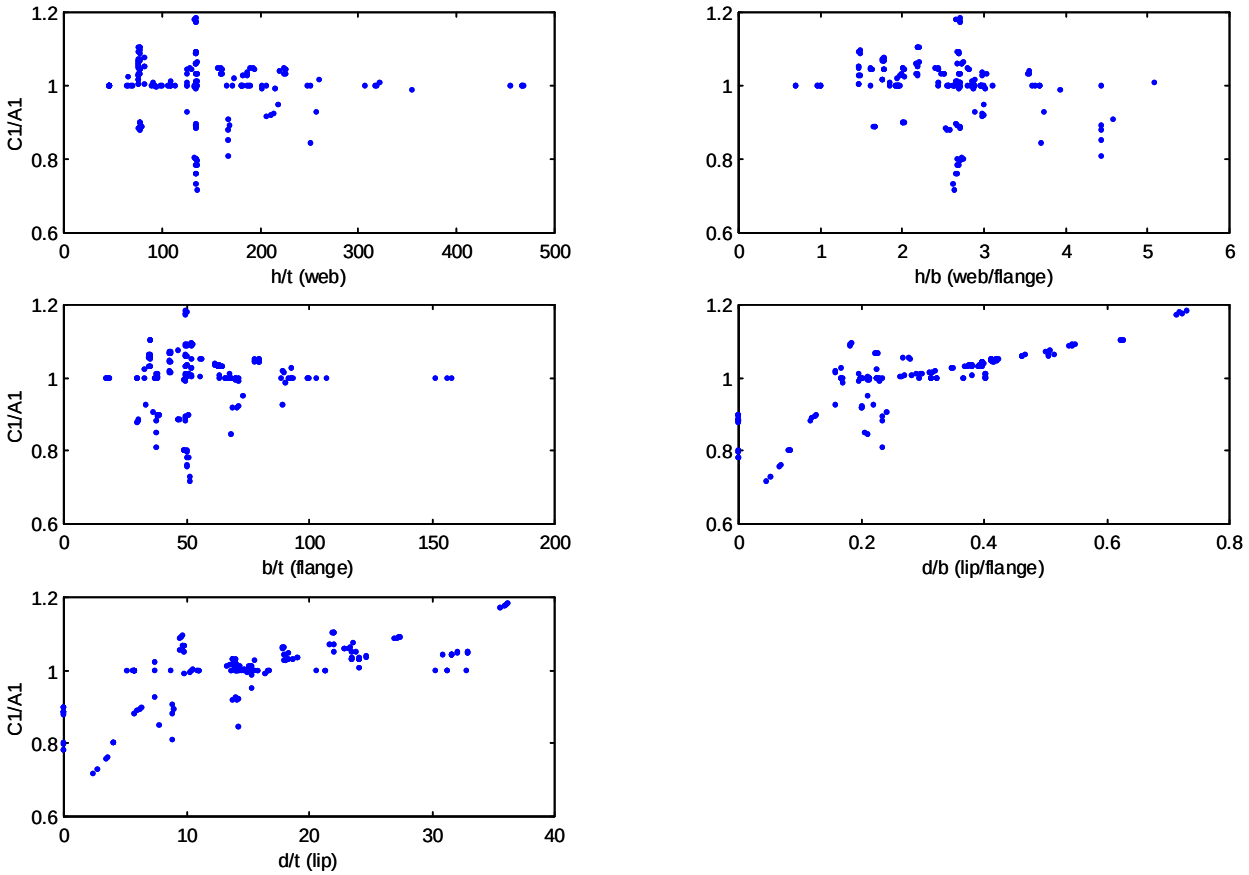

Figure 34 Impact of Adopting Proposal 2 an Alternative Effective Width Method, Shown as Ratio of Proposal 2 (C1) / AISI (A1) for the Lipped Channels and Z's Studied in this Report

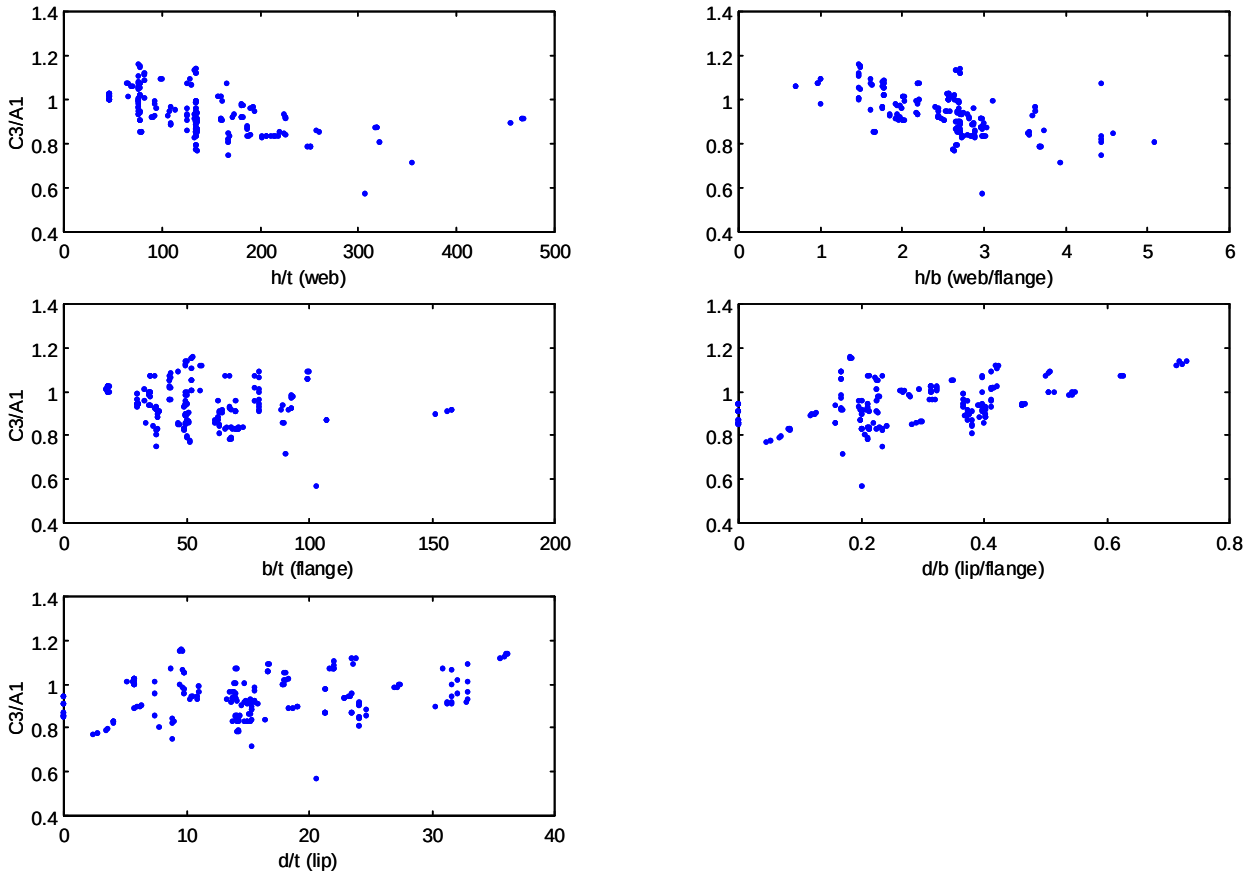

Figure 35 Impact of Adopting Proposal 3 the Direct Strength Method, Shown as Ratio of Proposal 3 (C3) / AISI (A1) for the Lipped Channels and Z's Studied in this Report

11 Conclusions

Ultimate strength of columns failing in the distortional mode is worthy of attention because distortional failures have lower post-buckling capacity than local modes of failure, distortional buckling may control failure even when the elastic distortional buckling stress (load) is higher than the elastic local buckling stress (load), and distortional failure modes have higher imperfection sensitivity. Existing experimental data demonstrates that if the failure is known to occur in the distortional mode, then the elastic distortional buckling stress (load) may be used to predict the ultimate strength.

Local buckling is the most common failure mode for the majority of existing lipped C and Z section columns. This is due to the fact that these members have slender webs, and as a result local buckling is a more common limit state than distortional buckling. Rack sections and other members with *h/b* ratios around 1, members with intermediate stiffeners in the web, and members with particularly small edge stiffeners, are all examples of columns that are prone to distortional failures. For these members explicit checks on distortional buckling are required for successful design.

The current AISI Specification provides a reasonable average prediction of standard lipped C and Z sections (on average nominal strength prediction is 6% unconservative). However, the AISI Specification exhibits systematic error for members with high *h/t* ratios (slender webs) and high *h/b* ratios (slender web with narrow flange). Further, AISI Specification predictions for tested Z sections over-predict the strength capacity of intermediate length edge stiffeners, and under-predict the strength capacity of long edge stiffeners. Issues related to local web/flange interaction, not distortional buckling are the primary source of errors in the AISI Specification. The addition of a simple distortional buckling check on top of existing AISI Specification rules does not remove the errors. Based on

these findings commentary language addressing the limits of the current AISI (1996) Specification is suggested for immediate adoption (see Appendix F.1).

A variety of alternative methods are shown to provide predictions that are as good or better than current design rules. However, design methods that continue the current effective width methodology of performing calculations separately for each element inherently suffer from an inability to consider the interaction of elements in local buckling. Nonetheless, since this is the currently accepted design procedure a method based on the effective width approach that properly incorporates distortional buckling was determined. This method (method C1 in Appendix D) is given in Appendix F.2 and is suggested for interim adoption into the AISI Specification.

The Direct Strength method (method C2 and C3 in Appendix D) given in Appendix F.3 is suggested as a long term solution for column design. Advantages of the Direct Strength method include: calculations do not have to be performed for individual elements, interaction of the elements in both local and distortional buckling is accounted for, distortional buckling is explicitly treated as a unique limit state, an obvious means for introducing rational analysis through numerical prediction of elastic buckling is provided, and a rational analysis procedure is provided for members with stiffener configurations or other geometries that current rules do not apply to. The Direct Strength method removes systematic errors that exist in the current AISI (1996) method. The method provides a means for integrating known behavior into a straightforward design procedure and will increase innovation of cold-formed steel member cross-sections.

12 References

American Iron and Steel Institute (1996). Cold-Formed Steel Design Manual. *American Iron and Steel Institute*.

Baldassino, N., Hancock, G. (1999). "Distortional Buckling of Cold-Formed Steel Storage Rack Section including Perforations."

Desmond, T.P. (1977). The Behavior and Design of Thin-Walled Compression Elements with Longitudinal Stiffeners. Ph.D. Thesis, Cornell University, Ithaca, New York.

Hancock, G.J., Kwon, Y.B., Bernard, E.S. (1994). "Strength Design Curves for Thin-Walled Sections Undergoing Distortional Buckling". *J. of Constructional Steel Research*, Elsevier, 31(2-3), pp. 169-186.

Hancock, G.J., Rogers, C.A., Schuster, R.M. (1996). "Comparison of the Distortional Buckling Method for Flexural Members with Tests." *Proceedings of the Thirteenth International Specialty Conference on Cold-Formed Steel Structures*, St. Louis, Missouri.

Kwon, Y.B., and Hancock, G.J., (1992) "Strength Tests of Cold-Formed Channel Sections undergoing Local and Distortional Buckling",*Jour Struct Engg,* ASCE, 117(2),, pp 1786 – 1803.

Lau, S.C.W., and Hancock, G.J (1987).,"Distortional Buckling Formulas for Channel Columns", *Journal of Structural Engineering*,ASCE,1987, 113(5), pp 1063 – 1078.

Loughlan, J. (1979). Mode Interaction in Lipped Channel Columns under Concentric or Eccentric Loading. Ph.D. Thesis. University of Strathclyde, Glasgow.

Miller, T.H., Peköz, T. (1994). "Load-Eccentricity Effects on Cold-Formed Steel Lipped- Channel Columns." *J. of Struct. Eng.*, ASCE, 120(3), pp. 805-823.

Mulligan, G.P. (1983). The Influence of Local Buckling on the Structural Behavior of Singly-Symmetric Cold-Formed Steel Columns. Ph.D. Thesis. Cornell University. Ithaca, New York.

Peköz, T. (1987). *Development of a Unified Approach to the Design of Cold-Formed Steel Members.* American Iron and Steel Institute Research Report, CF 87-1.

Polyzois, D., Charnvarnichborikarn, P. (1993). "Web-Flange Interaction in Cold-Formed Steel Z-Section Columns". *J. of Struct. Eng.* ASCE, 119(9), pp. 2607-2628.

Schafer, B.W. (1997). Cold-Formed Steel Behavior and Design: Analytical and Numerical Modeling of Elements and Members with Longitudinal Stiffeners. Ph.D. Thesis. Cornell University. Ithaca, New York.

Schafer, B.W., Peköz, T. (1998). "Direct Strength Prediction of Cold-Formed Steel Members using Numerical Elastic Buckling Solutions." *Fourteenth International Specialty Conference on Cold-Formed Steel Structures.* St. Louis, Missouri.

Schafer, B.W., Peköz, T. (1999). "Laterally Braced Cold-Formed Steel Flexural Members with Edge Stiffened Flanges." *Journal of Structural Engineering*. 125(2).

Thomasson, P. (1978). "Thin-walled C-shaped Panels in Axial Compression". *Swedish Council for Building Research.* D1:1978, Stockholm, Sweden.

American Iron and Steel Institute

1140 Connecticut Avenue, NW
Suite 705
Washington, DC 20036

www.steel.org

Research Report RP-00-1